Genome analysis and description of *Tunturibacter* gen. nov. expands the diversity of *Terriglobia* in tundra soils

Adriana Messyasz [1], Minna K. Männistö [2], Lee J. Kerkhof [3], and Max M. Häggblom [1*]

[1] Department of Biochemistry and Microbiology Rutgers University, 76 Lipman Drive, New Brunswick, NJ 08901, U.S.A.

[2] Natural Resources Institute Finland, Ounasjoentie 6, FI-96200 Rovaniemi, Finland

[3] Department of Marine and Coastal Sciences, Rutgers University, 71 Dudley Rd, New Brunswick, NJ 08901, U.S.A.

Running title: *Tunturibacter* gen. nov. in the *Acidobacteriota* phylum

Corresponding author:
Max M. Häggblom
haggblom@rutgers.edu

Abstract

Higher temperatures in Arctic tundra ecosystems are driving increased microbial respiration of soil organic matter with the release of carbon dioxide and methane. To understand the impacts of such microbial activity, we need to better characterize the complex diversity of Arctic soil microbial communities. Our aim is to refine the phylogenetic diversity of the ubiquitous, but elusive, members of the *Terriglobia* in the *Acidobacteriota* phylum so we can begin to link this diversity to differences in carbon and nitrogen utilization patterns. Long-read Oxford Nanopore MinION sequences were combined with metagenomic short-read sequences to assemble full *Acidobacteriota* genomes, build multi-locus phylogenies, and annotate pangenome markers to differentiate *Acidobacteriota* strains from several tundra soil isolates. We identified a phylogenetic cluster which contains four novel species previously associated with *Edaphobacter lichenicola* and conclude that the cluster represents a novel genus, *Tunturibacter*. Four novel species are described: *Tunturibacter lichenicola* comb. nov., *Tunturibacter empetritectus* sp. nov., *Tunturibacter gelidoferens* sp. nov., and *Tunturibacter psychrotolerans* sp. nov. By uncovering novel species and strains within the *Terriglobia* and improving the accuracy of their phylogenetic placements, we aim to enhance our understanding of this complex phylum and elucidate the mechanisms which shape microbial communities in polar soils.

Keywords: *Acidobacteriota,* soil isolates, genome assembly, MinION sequencing

INTRODUCTION

Approximately one-third of the global soil carbon stock is stored in Arctic soils (Loya and Grogan, 2004; Hugelius *et al.*, 2014), and despite sub-zero temperatures, microbial activity persists throughout the long winters, albeit at a slower rate (Oechel *et al.*, 1997; Welker *et al.*, 2000; Natali *et al.*, 2014; Nikrad *et al.*, 2016; Gadkari *et al.*, 2020; Pessi *et al.*, 2022; Poppeliers *et al.*, 2022). Microbes play important roles in nutrient cycling as they decompose soil organic matter (SOM). As polar soils warm due to climate change, it is of concern that enhanced microbial activity will increase the rate of SOM degradation and consequently greenhouse gas emissions (Welker *et al.*, 2000; Campbell *et al.*, 2010; Graham *et al.*, 2012; Natali *et al.*, 2014). SOM degradation usually increases in the short summer season, with climate change resulting in faster and longer soil decomposition and increased greenhouse gas emissions that contribute to a positive warming feedback loop (Schuur *et al.*, 2008; Bond-Lamberty and Thomson, 2010; Koven *et al.*, 2011). However, the mechanisms by which climate change affects gas emissions are complex and site specific, likely determined by e.g. vegetation type and microbial community structure (Fry *et al.*, 2023).

The microbial community diversity of Arctic environments, like the tundra, is shaped by soil abiotic factors (e.g., pH, SOM, temperature and water activity) and the extreme conditions of the Arctic (e.g., intense UV radiation, drought, long periods of sub-zero temperatures interspersed by freeze-thaw events) (Weintraub and Schimel, 2003; Männistö *et al.*, 2009; Tveit *et al.*, 2014; Taş *et al.*, 2018; Viitamäki *et al.*, 2022). Despite these harsh conditions, there is tremendous bacterial diversity in tundra soils, with the bacterial communities dominated by *Acidobacteriota*, *Actinomycetota* and *Pseudomonadota* (*Proteobacteria*) (Männistö *et al.*, 2007, 2013; Chu *et al.*, 2010; Kim *et al.*, 2014; Voříšková *et al.*, 2019; Viitamäki *et al.*, 2022). Members of these phyla change in abundance, composition, and activity in response to environmental variables such as seasonal changes (freeze-thaw cycles), vegetation, and soil pH (Männistö *et al.*, 2009, 2013; Zinger *et al.*, 2009; McMahon *et al.*, 2011; Viitamäki *et al.*, 2022). The ubiquitous but elusive *Acidobacteriota* are particularly susceptible to changes in soil pH and different members of the phylum thrive at different pH levels. Members of the Class *Terriglobia* (formerly *Acidobacteriia*; Subdivision 1 (SD1) *Acidobacteriota*) are

particularly abundant in the cold, nutrient poor, acidic soils such as those in Arctic tundra and boreal forest biomes (Männistö *et al.*, 2007, 2009; Campbell *et al.*, 2010; Kim *et al.*, 2014; Männistö *et al.*, 2018; Belova, Ravin, *et al.*, 2018; Ivanova *et al.*, 2020).

The *Acidobacteriota* is one of the most abundant phyla in soils around the globe, however the diversity within this phylum is still largely uncharacterized (Zhang *et al.*, 2022). Initial culture-independent methods initially delineated 26 subdivisions of *Acidobacteria* (Barns *et al.*, 2007). More recently, these subdivisions were refined into 15 class-level units (Dedysh and Yilmaz, 2018). Of these, the classes *Terriglobia*, *Blastocatellia* and *Vicinamibacteria* are most abundant in soils (Janssen, 2006; Jones *et al.*, 2009). Furthermore, members of the *Terriglobia* have been the most successfully cultivated group with over 40 named and published species to date (Zhang *et al.*, 2022; Göker, 2023).

The family *Acidobacteriaceae* currently encompasses over a dozen named genera, however with faster and more advanced sequencing technologies a greater number of *Acidobacteriota* species and strains are being described (Kalam *et al.*, 2020; Zhang *et al.*, 2022). The analysis of multiple genes from isolate genomes and environmental metagenomes has contributed towards a better understanding of the diversity of *Acidobacteriota* in multiple ecosystems without the need for cultivation (Parsley *et al.*, 2011; Kielak *et al.*, 2016; Kalam *et al.*, 2020; Dedysh *et al.*, 2022). Genome analysis has indicated a variety of metabolic functions within the *Acidobacteriota* including complex carbohydrate degradation (xylan, cellulose, hemicelluloses, pectin, starch, and chitin), nitrogen metabolism (nitrate, nitrite, and nitric oxide reduction), genes for oxygen utilization in hypo- and hyperoxic conditions, as well as the ability to oxidize methanol (Eichorst *et al.*, 2007; Ward *et al.*, 2009; Rawat *et al.*, 2012; Diamond *et al.*, 2019; Kalam *et al.*, 2020). Some *Acidobacteriota* are equipped with regulatory genes in response to stressors like starvation, oxidative stress, heat stress, as well as acid resistance systems (Ward *et al.*, 2009; Challacombe *et al.*, 2011; Kielak *et al.*, 2016; Kalam *et al.*, 2020). Secondary metabolites from biosynthetic gene clusters were also found within *Acidobacteriota*. Specifically, nonribosomal peptide synthetases and polyketides synthases were found within *Candidatus* Angelobacter (a

proposed *Terriglobia*), indicating mechanisms for interbacterial competition (Crits-Christoph *et al.*, 2022).

There may be several reasons for such a high taxonomic and functional diversity of *Acidobacteriota* in terrestrial systems. Primarily, soils create complex and spatially/temporally heterogenous environments, with this disequilibrium ensuring that no one species dominates over others (Lennon *et al.*, 2012; Ghoul and Mitri, 2016). Additionally, ecological drivers, such as resource partitioning, selective predation, and temporal separation, most likely shape the diversity of *Acidobacteriota* and other soil phyla (Chesson and Huntly, 1997; Chesson, 2000). To better understand how *Acidobacteriota* activity is shaped by environmental and ecological factors we need to identify the yet uncharacterized species/strains within this phylum and compare their genomes to elucidate metabolic potential. In this study, we sequenced several new tundra soil *Acidobacteriota* isolates from Malla Nature Reserve, Kilpisjärvi, Finland using both Illumina short-read and Oxford Nanopore long-read technologies. Through rRNA operon and full genome analysis we expand the current phylogenetic diversity of the order *Terriglobales* in the *Acidobacteriota.* We also delineate and name a novel genus, *Tunturibacter,* containing four new species in phylogenetic proximity to other species within the genera *Terriglobus* (Eichorst *et al.*, 2007; Männistö *et al.*, 2011; Rawat *et al.*, 2012; Podar *et al.*, 2019)*, Granulicella* (Pankratov and Dedysh, 2010; Männistö *et al.*, 2012; Rawat *et al.*, 2013, 2014), and *Edaphobacter* (Koch *et al.*, 2008; Wang *et al.*, 2016). With functional annotation and comparison of this new genus to known *Acidobacteriota,* the core and unique genes of the genera within this group can be identified. Our phylogenetic analysis demonstrates that a complex diversity of the *Terriglobales* can be uncovered. Additionally, understanding how novel genera differ within *Acidobacteriota* can help further elucidate why such diversity exists in soil environments.

EXPERIMENTAL PROCEDURES

Acidobacteriota isolation and DNA extraction

Acidobacteriota strains were isolated from tundra soil samples collected from Malla Nature Reserve, Kilpisjärvi, Finland (69°01′N, 20°50′E) in July 2010 (strain codes

that begin with “M”) and July 2012 (strain codes that begin with “X”). Several carbon substrates were tested in an attempt to isolate novel members of the *Acidobacteriota*.
141 Soil samples were diluted in VL55 mineral medium (Davis *et al.* 2005) and dilution plated on the different media. Plates were incubated at 4°C for up to three months and inspected every two weeks. To isolate *Acidobacteriota* and other slow growing
144 oligotrophs, only colonies that formed after 1-2 month incubation were picked and streaked to new media. After purification, isolated strains were identified by Sanger sequencing of the 16S rRNA gene. DNA was extracted from the isolates using the
147 DNeasy UltraClean Microbial Kit (Qiagen) according to the manufacturer’s instructions. 16S rRNA genes were amplified using 27f and 1525r primers (Lane *et al*., 1991) and the PCR products sequenced by LGC Genomics (Berlin, Germany) using the forward
150 primer 27f. Approximately 800 bp sequences were compared to those in the EzTaxon database (Yoon *et al*., 2017) and those identified as members of the *Acidobacteriota* selected for further studies.

153 Strains M8UP20, M8UP22, M8UP23, M8UP27, M8UP28, M8UP30, and M8UP39 were isolated using a mixture of carboxy methyl cellulose, xylan, pectin and starch (each 0.25 g l^{-1}) in VL55 mineral salt medium amended with yeast extract (0.1 g l^{-1}) and
156 agar (20 g l^{-1}). Strain MP8S11 was isolated using cellobiose, trehalose and sucrose (each 0.25 g l^{-1}) in VL55 mineral salt medium amended with yeast extract (0.1 g l^{-1}) and agar (20 g l^{-1}). Strains X4BP1, X5P3, X5P6, and X4EP2 were isolated using xylan (0.5
159 gl^{-1}, cellobiose (0.25 g l^{-1}) and xylose (0.25 g l^{-1}) in VL55 mineral salt medium amended with MEM essential and non-essential amino acids (Sigma-Aldrich®). VL55 mineral salt solution was prepared as described by Davis *et al*. (2005), pH was adjusted either to 4.0
162 or 5.5. All strains were maintained at pH 5.5 using GY medium containing glucose (1 g l^{-1}) and yeast extract (0.5 g l^{-1}) in VL55. Isolation of *Granulicella arctica* MP5ACTX2 has been described earlier (Männistö *et al.*, 2012).

165

Phenotypic and chemotaxonomic analyses

Growth of strains M8UP23, M8UP39 and X5P6 on GY medium was tested at
168 different temperatures and pH. Temperature range was evaluated by growth on GY-agar incubated at 2, 4, 10, 15, 20, 25 and 30°C. The plates were checked every 1-2

days for growth. Visual differences in growth at different temperatures were recorded.
171 The effect of pH on growth was evaluated by growing the strains in liquid GY medium at pH 3.0-9.0 (in 0.5 pH unit increments) in 96 well plates. Carbon source utilization of the three strains was analyzed in 96-well plates for up to 10 days at 20°C with VL55 mineral
174 medium supplemented with 100 mg l^{-1} yeast extract and 10 mM of each carbon source. Yeast extract was required for good growth on single carbon sources. The control contained only yeast extract. Growth was measured at 620 nm using a Multiscan FC
177 microplate reader (Thermo Scientific). Hydrolysis of different polysaccharides (starch, carboxy methyl cellulose (CMC), xylan, lichenan, pectin, xanthan and gum arabic) was determined at room temperature by observing CO_2 production for up to 20 days and
180 analyzed as described in Männistö et al. (2012).

Cellular fatty acids were analyzed by gas chromatography as described in Männistö et al. (2012). Analysis of respiratory quinones and polar lipids were carried out
183 by the Identification Service, DSMZ, Braunschweig, Germany. For the analysis, cells were cultivated on GY medium, collected by centrifugation, washed with PBS buffer, and freeze-dried. Polar lipids were extracted from 200 mg of freeze-dried cells and
186 separated by thin-layer chromatography (German Collection of Microorganisms and Cell Cultures GmbH: Polar Lipids). Respiratory quinones were extracted from 50 mg of freeze-dried cells and analysed by HPLC (German Collection of Microorganisms and
189 Cell Cultures GmbH: Respiratory Quinones).

Genome sequencing and assembly

192 A total of 13 *Acidobacteriota* isolates were used for whole genome sequencing via the Oxford Nanopore MinION. Sequence libraries were prepared using R 9.4 chemistry and the MinION Rapid Sequencing kit (SQK-RAD004). Libraries were run on
195 a MinION R9.4 Flongle for approximately 24 hours. Fast5 files were basecalled using Guppy (V 6.0.1) (Oxford Nanopore Technologies Ltd.) in high accuracy mode and the FastA reads were used for genome assembly with the Trycycler assembler package (V
198 0.5.3) (Wick *et al.*, 2021), which allows for multiple assemblies specific to Nanopore long read sequences. For these genomes, the assemblers Flye --nano-hq (V 2.9) (Lin *et al.*, 2016; Kolmogorov *et al.*, 2019), Minipolish (V 0.1.2) (Wick and Holt, 2019), and

Raven (V 1.8.1) (Vaser and Šikić, 2021) were employed using default settings. The contigs were put into clusters and multiple sequence alignments were generated to produce a consensus or final assembly using Medaka (V 1.6.0) (© 2018 Oxford Nanopore Technologies Ltd.).

In addition, several of the assemblies were run through PolyPolish (V 0.5.0) (Wick and Holt, 2022) to close and complete the genomes. Of the 13 isolates used for genome assembly, 6 also had Illumina short-read sequences publicly available via the JGI Genome Portal (see Project IDs in Table S1), and 4 (MP8S11, M8UP39, X5P6, and M8UP23) were previously sequenced via Illumina (Supplemental Methods and Results). These short reads along with our Trycycler-Medaka assemblies were used in the PolyPolish pipeline (default parameters). Genome assembly completeness and contamination for all 13 isolates was analyzed via CheckM (V 1.0.18) (Parks *et al.*, 2015). Percent GC was calculated via QUAST (V 4.4) (Gurevich *et al.*, 2013). For each assembly with greater than one contig, the second longest contig was searched against the plasmid database PLSDB (V 2023_11_03_v2) (Schmartz *et al.*, 2021). This search was conducted via the PLSDB online API tool using Mash (V 2.3) (Ondov *et al.,* 2016) to search against the PLSDB database (parameters used: maximal p-value 0.1, maximal distance 0.1, minimal identity 0.70). Gene prediction was run via Prokka (V 1.14.5) (Seeman 2014). To find annotations to Carbohydrate-Active Enzymes (CAZy), genes annotated via Prokka were scanned using a set of Hidden Markov Models (HMMs) from the dbCAN2 CAZy collection (dbCAN HMM database v10) (Zhang *et al.,* 2018) using HMMER (v 3.3.2) (Eddy, 2011). The minimum e-value for this search was 1e-15 and the minimum coverage of the model length was set at 90%. The Genome Taxonomy Database (GTDB; releases 207 and 214; GTDB R07-RS207 and R08-RS214) (Parks *et al.*, 2022) was used to taxonomically classify the genomes via the GTDB-Tk tool (v 2.3.2).

Genome phylogenies and pangenome analysis

A single copy gene (SCG) phylogeny including the 13 new tundra soil isolate genomes and known Class *Terriglobia* (SD1 *Acidobacteriota*) species was analyzed via the GToTree program (V 1.7.05) (Lee, 2019). The program was run with default settings

for alignment (MUSCLE V 5.1) (Edgar, 2021) and approximately-maximum-likelihood phylogenetic tree building (FastTree V 2.1.11) (Price *et al.*, 2010). The "-H Bacteria" parameter was used to identify 74 bacterial single copy genes across all genomes analyzed (listed in Supplementary Materials). Another multi-locus tree for the same genomes was built via OrthoFinder (V 2.5.4) (Emms and Kelly, 2019). The Orthofinder tree also utilized a MUSCLE (V 5.1) (Edgar, 2021) alignment and phylogenetic tree building with FastTree (Price *et al.*, 2010). Both SCG and OrthoFinder trees were viewed via the iTOL interface (V6) (Letunic and Bork, 2021). These trees were compared to 16S rRNA gene and rRNA-operon trees, which included a more complete representation of the *Terriglobia* and the novel *Acidobacteriota* isolates included in the rRNA operon analysis (see Supplementary Methods and Results). Genome alignment visualizations were conducted via PGV-Mummer (default setting; V 0.3.2) (Shimoyama, 2022) and progressive MAUVE (Geneious plugin V 1.1.1) with 15 match seed weight, minimum 5,000 Locally Collinear Blocks (LCB) score, full alignment, and MUSCLE 3.6 gapped aligner (Darling *et al.*, 2004).

Genome assemblies of the new tundra isolates along with some select *Terriglobia* were further compared through the Anvi'o pangenome analysis pipeline (Eren *et al.*, 2021). A contig database for each genome was created with the following additions: HMM search, SCG taxonomy, tRNAs scan, NCBI cogs search, and KEGG Kofam search. Average nucleotide identity across the compared genomes was calculated via pyANI (Pritchard *et al.*, 2015) program plugin within the Anvi'o pangenome pipeline (command: "anvi-compute-genome-similarity"). The pangenome was then visualized via the Anvi'o interactive display, organizing samples by a gene cluster frequencies tree. Functional enrichment between strain categories within the pangenome analysis was computed via anvi-compute-functional-enrichment-in-pan using the KEGG_Class and COG20_PATHWAY annotation sources (Shaiber *et al.*, 2020).

Analysis of *Acidobacteriota* community in Malla tundra heath soils

Soil samples were collected from tundra heaths of Mt. Pikku Malla in Malla Nature Reserve, Kilpisjärvi (69°03' 50"N, 20°44'40"E), with differences in topography

that dramatically influence snow accumulation. Four plots representing windswept slopes and four plots corresponding to snow-accumulating biotopes were sampled at a depth of <5 cm in February 2013 as described previously (Männistö *et al*. 2024). Composite soil samples of 5 soil cores were taken from each plot with three subsamples from each composite sample used for DNA extraction with a CTAB-based method.

Near full-length bacterial rRNA operons were amplified from extracted DNA using 16S rRNA-27Forward and 23S rRNA-2241R primers, <10 ng template DNA, and a High-Fidelity Taq Polymerase (Biomake Inc., CA, USA; Kerkhof *et al*., 2017). PCR conditions were: Initial denaturation for 3 min at 94°C; followed by 25 cycles of 98°C/10 sec denaturation, 60°C/15 sec primer annealing and 72°C/240 sec extension; and a final extension at 72°C for 5 min. Barcoded rRNA operon amplicons were visualized and quantified by agarose gel electrophoresis and stored at -20°C until library preparation. Library construction utilized the SQK-LSK108 sequencing kit and sequencing via the Oxford Nanopore MinION. The fast5 files were basecalled using Guppy (3.2.0). Raw reads were demultiplexed with Guppy and sized (3700-5000 bp) using Geneious (11.1.5). FastA files were initially screened via MegaBLAST (2.10.0) against the ribosomal RNA operon database (rOPDB; Kerkhof *et al*., 2022) to determine the raw reads associated with the *Acidobacteriota*. These *Acidobacteriota* reads were re-screened against a modified database using the original *Acidobacteriota* rRNA operons from the rOPDB, amended with rRNA operons from the new *Tunturibacter* and *Granulicella* strains described in this study. Best BLAST hits (BBHs) were identified using the following settings: word size -60, match/mismatch cost -2/-3, gap open/extend -0/−4, and e-value of $1x10^{-10}$. Relative abundance of the *Acidobacteriota* BBHs to the updated database was calculated and bubble plots were generated in RStudio (2023.06.0+421) using ggplot2 and reshape2.

RESULTS AND DISCUSSION

Novel tundra *Acidobacteriota* isolates

Acidobacteriota strains were isolated from tundra heath soil samples from Malla Nature Reserve using different carbon substrate combinations. Initial analysis of partial 16S rRNA sequences (data not shown) indicated that these were members of the *Terriglobia*, closely related to *Edaphobacter* and *Granulicella* species. Physiological comparisons of our isolates to known *Edaphobacter* and *Granulicella* strains showed similarities in the utilization of various organic compounds and slight differences in temperature and pH range. Further investigation utilizing long-read Oxford Nanopore sequencing to assemble full genomes uncovered phylogenetic differences between the isolates and other members of the *Terriglobia.* The consistent phylogenetic placement across several comparative tools (single-gene trees, multi-locus trees, pangenome analysis) clearly separates the tundra heath isolates from known *Edaphobacter* and *Granulicella* species. Therefore, these isolates ultimately represent a novel genus within *Terriglobia* for which we propose the name *Tunturibacter*. Here we present the genomic, phylogenetic, and phenotypic characterization of four novel species within the *Tunturibacter* genus.

Genome assemblies

The 13 new *Acidobacteriota* genome assemblies are listed in Table 1. Of these, 10 included Illumina short reads used to polish the genomes to >99% completion. Three of the 10 complete genomes had only one scaffold/contig, while the remainder had two or more scaffolds/contigs, with the longer scaffold representing the bacterial chromosome and the shorter contigs representing smaller genetic elements, i.e. plasmids. To examine whether these shorter contigs could be plasmids, we searched the shorter contigs from assemblies with more than one contig against the PLSDB plasmid database. For each assembly, the second longest contig had one or more hits with an average 75% identity to an already annotated plasmid from the database (Table S2). Their predominant alignment to plasmids from *Granulicella tundricola* at only around 75% identity indicates these are novel plasmids belonging to the *Tunturibacter.* These plasmids may code for a few extra genes that are not necessary for *Tunturibacter* growth, reproduction, or existence, but may offer some resistance strategies beneficial for survival.

The assembled genomes of the *Tunturibacter* strains had between 3,600-7,400 predicted genes, of which >98% were protein coding genes for each assembly (Table 1). Of these genes, on average approximately 44% were annotated as non-hypothetical. Full assembly statistics for these genomes are included in Table S1. Based on GTDB annotation, 10 out of 13 assemblies were classified as most similar to *Edaphobacter lichenicola* DSM 104462 with ANI values ranging from 89% to 100% and amino acid (AA) similarities from 76% to 94%. Of the remaining three assemblies, two were classified as most similar to *Granulicella arctica* MP5ACTX2 (DSM 23128) (79%-100% ANI and 86%-94% AA) and one to *Granulicella mallensis* MP5ACTX8 (100% ANI and 94% AA).

Multi-locus phylogeny of the SD1 *Acidobacteriota*

To determine the taxonomic placement of the new tundra *Acidobacteriota* isolates we compared 16S rRNA gene, rRNA operon, and single copy gene phylogenies. Utilizing the full genomes of members of the *Terriglobia*, we phylogenetically compared the genome assemblies using 74 selected single copy genes (SCGs) (Figure 1A). The resulting SCG tree more accurately groups the *Edaphobacter*, *Granulicella* and *Terriglobus* species than the rRNA operon or 16S rRNA gene trees alone (Figures S1A-B and S2A-B). Importantly, the assemblies grouping together with *Edaphobacter lichenicola* DSM 104462 were phylogenetically separated from the other *Edaphobacter* species, including the type species *E. modestus*, and would thus represent the new genus *Tunturibacter*. As can be seen from the SCG tree, this new genus appears to comprise four species, each with several strains.

The phylogeny is more evident in the SCG sub-tree showing the members of the *Terriglobia* most closely related to the proposed *Tunturibacter* genus (Figure 1B). The SCG tree also more accurately clusters the *Granulicella* species. Another potential new genus may be represented by *Granulicella mallensis, G. paludicola,* and *G. cerasi,* which group with *Bryocella elongata*, phylogenetically distinct from the other species in the *Granulicella* cluster, including the type species *G. paludicola* (Figure 1A). A comparison of these genomes via a multi-locus phylogeny based on orthogroups and

orthologs (Orthofinder) also resulted in a similar phylogenetic structure as the SCG tree (Figure S3).

Overall, compared to the rRNA operon tree, phylogenies built on multiple genes from fully assembled genomes more accurately delineated the *Acidobacteriota* genera and species. However, the rRNA operon tree was still able to differentiate the various novel clusters, revealing the polyphyletic nature of some of these genera, supporting the separation of *Edaphobacter lichenicola* and three new species as the proposed new genus *Tunturibacter.*

Pangenome Analysis

Pangenome analysis was used to compare gene frequencies from the COG, KEGG, SCG, and Kofam annotations of the input genomes (Figure 2 and Figure 3). The gene frequency tree created from this analysis (Figure 2, right side) is similar to the SCG tree, again supporting the separation of two new potential genera in the *Terriglobia*. The proposed *Tunturibacter* genus is present as its own cluster, as is the cluster which groups several *Granulicella* species that affiliate with *Bryocella elongata* (Figure 2). The very last row indicating the number of contributing genomes (Figure 2 bottom left) shows that the area of the pangenome comparison with the most contributing genomes also includes the SCG clusters, representing the core genome of the *Acidobacteriota* analyzed (Figure 3; Bin 1, 337 clusters, 11,791 gene calls).

With the exception of strain M8UP15, ANI analysis clearly separated the proposed new *Tunturibacter* species from the other *Edaphobacter* species, with *E. modestus* as the type species. The ANI similarities, along with the phylogenetic clusters of this new genus in the SCG tree (Figure 1) support the separation of four species within the new *Tunturibacter* genus with their respective type strains: *E. lichenicola* DSM 104462 transferred to the genus as *Tunturibacter lichenicola* comb. nov. (includes strain MP8S11), *Tunturibacter psychrotolerans* sp. nov. X5P6 (includes strains X4BP1 and X5P2), *Tunturibacter empetritectus* sp. nov. M8UP23 (includes strains M8UP22, M8US30, M8UP20, and M8UP27), and *Tunturibacter gelidoferens* sp. nov. M8UP39 (includes strains M8UP30 and M8UP28). Bin 2 captures the gene clusters unique to this new genus (Figure 3; Bin 2, 147 clusters, 1,903 gene calls).

One major difference in this analysis compared to the SCG tree, is the grouping of genome M8UP15 with *E. aggregans* DSM 19364 rather than the *Tunturibacter* genus. These two genomes have the highest number of gene clusters, with one area sharing multiple genes unique to these two genomes (Figure 3; Bin 3, 1,820 clusters, 3,640 gene calls). The high ANI similarity of these two genomes indicates that strain M8UP15 is most closely related to *E. aggregans* DSM 19364. However, out of all the genomes in this analysis, M8UP15 and *E. aggregans* DSM 19364 share the highest number of partial genes (416), indicating that their genomes are not complete. Since the SCG and operon trees did not group these two genomes closely, it is unclear whether this result is being driven by their unique genes or their incomplete genomes. The taxonomic placement of strain M8UP15 may thus require future reassessment.

Physiological comparison of *Tunturibacter* species

The phenotypic properties of the proposed type-strains for the new species, *Tunturibacter empetritectus* M8UP23, *Tunturibacter gelidoferens* M8UP39, and *Tunturibacter psychrotolerans* X5P6 were compared to *Tunturibacter* (*Edaphobacter*) *lichenicola* (Belova, Suzina, *et al.*, 2018). Similarities were found for all strains based on their utilization of various organic compounds (Table 2), as well as hydrolysis of polysaccharides, enzyme activities (API ZYM tests), and composition of quinones and major cellular fatty acids (Table S4). The temperature growth range for strains *T. empetritectus* M8UP23, *T. gelidoferens* M8UP39, and *T. psychrotolerans* X5P6 was 2-30°C, while the growth range of *T. lichenicola* DSM 104462 was different at 7-37°C. These *Tunturibacter* species/strains tolerate cold conditions, similar to *Terriglobus* (4-30°C) (Eichorst *et al.*, 2007; Männistö *et al.*, 2011) and *Granulicella* species (4-28°C) (Männistö *et al.*, 2012). The growth pH range for *T. empetritectus* M8UP23, *T. gelidoferens* M8UP39, and *T. psychrotolerans* X5P6 was 3.5-6.5 and for *T. lichenicola* DSM 104462 was 3.4-7.0. These ranges are most similar to those of *Granulicella tundricola* and *Granulicella mallensis* (pH 3.5-6.5) (Männistö *et al.*, 2011) and can tolerate more acidic conditions than *Terriglobus* (pH 4.5-7.5) (Eichorst *et al.*, 2007; Männistö *et al.*, 2012).

Genome comparisons of *Tunturibacter* species

Genome alignments at various taxonomic levels further support the designations of the new *Tunturibacter* species and strains (Figure 4). Only the longest assembled scaffold for each genome was used for the alignment. At the genus level we compared *Tunturibacter lichenicola* DSM 104462 (5,662,239 bp), *Granulicella arctica* DSM 23128 (4,736,692 bp), *Edaphobacter modestus* DSM 18191 (6,121,180 bp), and *Terriglobus saanensis* SP1PR4 (5,095,225 bp). At the species level we compared *Tunturibacter lichenicola* DSM 104462 (5,662,239 bp), *Tunturibacter empetritectus* M8UP23 (4,898,072bp), *Tunturibacter gelidoferens* M8UP39 (5,453,280bp), and *Tunturibacter psychrotolerans* X5P6 (5,619,635bp). At the strain level we also compared *Tunturibacter empetritectus* strains M8UP23 (4,898,072bp), M8UP20 (4,830,045bp), M8UP22 (5,076,618bp), and M8UP27 (4,842,676bp).

These alignments show decreased homology when comparing the *Tunturibacter* genomes against other genera in the *Terriglobia* (Figure 4A), compared to increased homology when comparing the genomes of the *Tunturibacter* species against each other (Figure 4B and 4C). The strength of homology increases with species and strain level alignments, with strain level alignments (within the *T. empetritectus* strains) showing the least amount of genome rearrangements (Figure 4C). These trends are also apparent when using another genome alignment visualization tool, Mauve (Figure S4A-C), which results in longer homology segments within alignments at the proposed strains compared to the species and genus level alignments.

Unique pathways and phenotypic data of *Tunturibacter* species

The *Tunturibacter* strains had between 3,600-7,400 predicted genes, of which >98% were protein coding genes (Table 1). All strains had at least one successful alignment to a gene family in the CAZy HMM database within the following CAZy classes: glycoside hydrolases, glycosyl transferases, carbohydrate-binding modules, carbohydrate esterases, polysaccharide lyases, and auxiliary activities. For each assembled genome the number of CAZy gene alignments includes one or more hits to unique CAZy genes spanning numerous functions (Table 1; Figure S5). In the different strains, 8 to 16% of the total number of predicted genes were code for modules of the

CAZy family, with genes for glycoside hydrolases being most abundant. While these hits represent mostly partial alignments to CAZy genes, this indicates a wide set of unique genes involved in the build-up and breakdown of complex carbohydrates.

Compared to the other *Acidobacteriota* genomes in the pangenome analysis, several pathways were significantly enriched ($p < 0.05$) in members of the *Tunturibacter* genus (Table 3). Based on KEGG Class and COG20 Functional annotations, *Tunturibacter* genomes are more enriched in functional pathways involving the metabolism of amino acids, such as tryptophan, betaine, and lysine. The enriched GABA (γ-aminobutyric acid) biosynthesis pathway suggests a pH resistance strategy within the *Tunturibacter* spp. (Dhakal *et al.*, 2012). This genus is also enriched in genes within pathways involving the metabolism and biosynthesis of cofactors and vitamins such as menaquinone, cobalamin, biotin, and molybdopterin. These (COG20 Pathway) annotations do not, however, support the presence of the full pathway within the *Tunturibacter.* The specific KEGG and COG20 genes annotated from the enriched functional pathways can be found in Table S5.

Additionally, there is a lack of evidence for prominent vitamin and cofactor biosynthesis genes within many members of the *Terriglobia*. Menaquinone has been found in *Acidobacterium capsulatum* (Kishimoto *et al.*, 1991), cobalamin (B12) transport has only been speculated in SD4 and SD8 *Acidobacteriota* and *Bryocella* species (Kielak *et al.*, 2016). An uncultivated group of *Acidobacteriota,* GAL08, from hot springs contained a biotin-specific transporter, however it was not able to synthesize biotin (Ruhl *et al.*, 2022). Although more detailed analysis is needed, the enrichment of vitamin/cofactor biosynthesis genes within the *Tunturibacter* suggests that members of this genus may be able to synthesize vitamins *de novo* and have increased metabolic capabilities compared to the *Edaphobacter, Granulicella,* and *Terriglobus* species.

Acidobacteriota community in Malla tundra heath soils

We examined the distribution of the *Terriglobia* in a set of snow-accumulating and windswept tundra heath soils in Malla Nature Reserve, from which the novel *Tunturibacter* species were isolated. At this site, areas in depressions are sheltered from the winds with high snow accumulation (up to ≥ 1m), while windswept areas

remain essentially snow-free throughout the winter leading to distinctly different soil temperature profiles and differences in the amplitude of annual temperature variation (Männistö *et al*., 2024). The bacterial communities were assessed by rRNA operon profiling with the Oxford Nanopore MinION, enabling strain-specific identification of bacterial community members. Overall, rRNA operon reads from the *Acidobacteriota* represented 4.2-18.4% of the >760K total bacterial reads from these tundra samples. Specifically, the *Acidobacteriota* reads varied from 1,524-18,818 reads per sample with an average of 6,536 ± 5,478 per site. Re-screening of these reads against the augmented *Acidobacteriota* rRNA database, containing the new rRNA operons from this study, indicated that 18-38% of these *Acidobacteriota* reads have best BLAST matches to *Tunturibacter* and *Granulicella.*

Furthermore, distinct differences in the relative abundance of *Edaphobacter*, *Granulicella* and *Terriglobus* species/strains could be observed between windswept and snow-accumulating tundra heaths (Figure 5). Reads matching to the various *Tunturibacter* strains were generally more dominant in the windswept plots, while *Granulicella* strain were more abundant in the snow-accumulating plots. These strain and species distinctions correspond to the observed differences in the overall soil microbial communities between windswept and snow-accumulating tundra heaths (Männistö *et al.,* 2024). Snow-cover and the linked vegetation shifts and soil C and N dynamics may thus be an important microclimatic driver of bacterial communities. The improved taxonomy of the *Acidobacteriota* combined with the genomic and phenotypic information of cultivated strains will enable and improved understanding of the community response to fluctuating environmental conditions in a changing climate.

Ecological context of *Acidobacteriota* in tundra soils

Members of the *Acidobacteriota* are ubiquitous in acidic Arctic tundra and sub-Arctic forest soils. The Kilpisjärvi study site has representative tundra vegetation dominated by dwarf shrub-rich *Empetrum* heaths over acidic soils, or forb- and graminoid-rich *Dryas* heaths over non-acidic soils (Männistö *et al.*, 2007, 2009, 2013; Eskelinen *et al.*, 2009). These soils are organic-rich and well-aerated, harboring abundant aerobic heterotrophic microbiota where diverse *Acidobacteriota* make up 10-

40% of the total bacterial community (Männistö *et al.*, 2009, 2013). The abundance and composition of the *Acidobacteriota* vary with topography and exposure that influence snow accumulation and soil temperatures (Männistö *et al.*, 2013) as well as bedrock material which influences soil pH (Männistö *et al.*, 2007). Different species within the *Acidobacteriota* appear to respond to environmental conditions differently, highlighting the wide functional diversity of these organisms even within the *Terriglobia*. From the tundra heath sites in Kilpisjärvi Finland, several species of *Terriglobus*, *Granulicella* and *Tunturibacter* have been cultivated (Männistö et al 2011, 2012, this study). These species appear adapted to breakdown, utilization and biosynthesis of diverse polysaccharides, and resilience to fluctuating temperatures and nutrient-deficient conditions.

Increased competition between plants and microbes and within the microbial community can occur due to environmental factors such as the increased presence of woody evergreen shrubs that immobilize nutrients as a consequence of warming-induced 'shrubification' on Arctic soil carbon storage (Stark *et al.*, 2023). Tundra soil carbon and nitrogen cycles are strongly coupled with soil nitrogen availability often decreasing over the growing season, leading to the soil microbial communities becoming increasingly N-limited (Jonasson *et al.*, 1999, Stark and Kytöviita, 2006). Methods to combat low nutrient concentrations include having the functional capacity for nutrient assimilation and transport. *Acidobacteriota* are known to contain genes involved in attaining nitrogen, which include genes essential for ammonia assimilation, e.g. glutamine synthetase, and genes for the ammonium channel transporter family (*amtB* gene) (Eichorst *et al.*, 2018). In a recent study comparing microbial responses to Arctic greening in Alaskan soils, *Acidobacteriota* most strongly expressed the glutamine synthetase metaprotein, a large component of the proteins involved in ammonia metabolism (Miller *et al.*, 2023). Within our study, glutamine synthetase (COG0174) was annotated mainly within the core genome of the *Tunturibacter* pangenome (Figure 3; Bin 1).

Another adaptation to low nutrient concentrations includes genes for high affinity transport systems (Kielak *et al.*, 2016; Eichorst *et al.*, 2018). Transporter genes annotated within the *Tunturibacter* pangenome include high affinity Mn^{2+} porin

(COG3659), high-affinity iron transporter (COG4393), and high-affinity nickel/cobalt permease (HoxN) (COG3376). *Acidobacteriota* have been shown to contain a broad substrate range of transporters, including the Drug/Metabolite transporter superfamily, the Ammonia Transporter Channel (Amt) Family, and the Metal Ion (Mn^{2+} Iron) Transporter (Nramp) (Kielak *et al.*, 2016). This diversity of transporters suggests that *Acidobacteriota* have an advantage in nutrient assimilation in nutrient poor conditions.

Tundra soil *Acidobacteriota* appear to be oligotrophs with slow growth rates and low population turnover rates that are favored by the presence of recalcitrant carbon. The genomes of the tundra soil *Acidobacteriota* contain an abundance of conserved genes/gene clusters encoding for modules of the carbohydrate-active enzyme (CAZyme) families, predominately glycoside hydrolases and glycosyltransferases (Figure S5; Rawat *et al.*, 2012; Eichorst *et al.*, 2018). In our study, pangenome glycosyltransferase COGs involved in cell wall biosynthesis (COG0438) and in the glycosylation of proteins and lipid IVA (COG1807) were found across all *Acidobacteriota* analyzed. Multiple alignments to various CAZy gene families were also found within the *Tunturibacter* indicating for a wide ability for utilizing complex carbohydrates. Another interesting feature of the *Acidobacteriota* is their synthesis of hopanoid lipids, which may play a role in regulating membrane stability. Additionally, quorum-sensing associated genes, such as acyl homoserine lactone (acyl-HSL), were found within several *Tunturibacter* and across *Acidobacteriota* within our pangenome analysis (Parsek *et al.,* 1999). Signaling molecules like acyl-HSLs are known to impact bacterial community dynamics in soils, particularly in response to virulence genes (Parsek *et al.,* 1999; Riaz *et al.,* 2008).

Members of the *Acidobacteriota* are known to play a role in decomposition of soil organic matter, in particular various biopolymers, and they participate in the global cycling of carbon, iron and hydrogen. While *Acidobacteriota* constitute from 5 to 50% of the total bacterial community in organic-rich, low pH, Arctic and boreal soils based on rRNA gene reads (Männistö *et al.*, 2007, 2009, 2013) they continue to be notoriously difficult to cultivate and are thus woefully under-represented in culture collections. The description of new strains and species provides key phenotypic and genomic information to help us understand why they are so dominant and how they maintain

diversity within the group. There is much to learn about their ecosystem functions in soils, their interactions with other microbes, and their adaptations to environmental stress and climate change.

Description of *Tunturibacter* gen. nov.

The results from the multiple lines of analyses presented above indicate that *E. lichenicola* is not a member of the genus *Edaphobacter* and should be reclassified as a species of the proposed new genus *Tunturibacter*, with the proposed name *Tunturibacter lichenicola* comb. nov. The NCBI BioProject ID for the 10 newly assembled *Tunturibacter* genomes is: PRJNA1004338. Accession numbers for all new Tunturibacter 16S rRNA genes and genomes are in Table S6.

Tunturibacter (Tun'tu.ri.bac'ter. tunturi, referring to the Arctic treeless fells in Finland, N.L. masc. n. *bacter*, a short rod; N.L. masc. n. *Tunturibacter* rod-shaped tundra fell bacterium).

Cells are Gram-negative aerobic rods. On agar plates, cells form circular, mucoid colonies. Colony pigment varies from light beige to pink. Produce extracellular polysaccharide-like substances. Sugars are preferred carbon sources and the different strains are capable of hydrolyzing various polysaccharides. The major cellular fatty acids are iso-15:0, iso-13:0, 16:1ω7c, 16:0. The predominant menaquinone is MK-8. The DNA G+C content is 56–58%. Strains have been isolated from tundra soil and lichen thalli collected from lichen-dominated forested tundra. The type species is *Tunturibacter lichenicola* comb. nov.

Emended description of *Tunturibacter lichenicola* comb. nov.

The description is as given by Belova et al. (2018). The type strain is SBC68^T (=DSM 104462^T =VKM B-3208^T).

Description of *Tunturibacter empetritectus* sp. nov.

Tunturibacter empetritectus (em.pet.ri.tectus. *empetri*, referring to the plant *Empetrum nigrum* ssp. *hermaphroditum*; L. adj. *tectus*, covered; L. part. Adj. *empetritectus*, growing under tundra heath dominated by *Empetrum nigrum* ssp. *hermaphroditum*).

Cells are Gram-negative, non-motile, aerobic rods. Colonies are light beige or pink, circular and smooth when grown on GY agar (Figure S6). Growth occurs at 2-30°C and at pH 3.5-6.5. In VL55 mineral medium with 100 mg l^{-1} yeast extract and 5–10 mM carbon source, utilizes cellobiose, xylose, fructose, fucose, glucosamine, glucose, L-glutamic acid (weak), maltose, mannose, N-acetyl-glucosamine, salicin and trehalose. Hydrolyzes xylan, pectin, xanthan and gum arabic. The major cellular fatty acids are iso-15:0, iso-13:0, 16:1ω7c, 16:0. The DNA G+C content determined from genome sequence of type strain is 57.82%.

The type strain is M8UP23^T (= DSMZ 117310 = HAMBI 3810) isolated from tundra soil in Malla Nature Reserve, Kilpisjärvi, Finland (69°01′N, 20°50′E). NCBI accession numbers for the 16S rRNA gene sequence and for the draft genome sequence of the type strain are OR449309 and CP132932-CP132934, respectively.

Description of *Tunturibacter gelidoferens* sp. nov.

Tunturibacter gelidoferens (ge.li.do.ferens. L. adj. *gelido* cold; L. pres. Part. *Ferens*, to endure; L. part. Adj. *gelidoferens*, cold-enduring).

Cells are Gram-negative, non-motile, aerobic rods. Colonies are pink, circular and smooth when grown on GY agar (Figure S6). Growth occurs at 2-30°C and at pH 3.5-6.5. In VL55 mineral medium with 100 mg l^{-1} yeast extract and 5–10 mM carbon source, utilizes cellobiose, xylose, fructose, fucose, glucosamine, glucose, L-glutamic acid (weak), maltose, mannose, N-acetyl-glucosamine, salicin and trehalose. Hydrolyzes carboxy methyl cellulose (weak), xylan, pectin, lichenin, starch (weak), and gum arabic (weak). The major cellular fatty acids are iso-15:0, iso-13:0, 16:1ω7c, 16:0. The DNA G+C content determined from genome sequence of type strain is 57.42%.

The type strain is M8UP39^T (= DSMZ 117311 = HAMBI 3809) isolated from tundra soil in Malla Nature Reserve, Kilpisjärvi, Finland (69°01′N, 20°50′E). NCBI accession numbers for the 16S rRNA gene sequence and for the draft genome sequence of the type strain are OR449311 and CP132937-CP132938, respectively.

Description of *Tunturibacter psychrotolerans* sp. nov

Tunturibacter psychrotolerans (*psy.chro.to'le.rans*. Gr. Adj. *psychros*, cold; L. pres. Part. *Tolerans*, tolerating; N.L. part. Adj. *psychrotolerans*, cold-tolerating).

Cells are Gram-negative, non-motile, aerobic rods. Colonies are light beige to light pink, circular and smooth when grown on GY agar (Figure S6). Growth occurs at 2-30°C and at pH 3.5-6.5. In VL55 mineral medium with 100 mg l^{-1} yeast extract and 5–10 mM carbon source, utilizes cellobiose, xylose, fructose, fucose, glucosamine (weak), glucose, L-glutamic acid (weak), maltose, mannose, N-acetyl-glucosamine (weak), salicin and trehalose. Hydrolyzes carboxy methyl cellulose (weak), pectin, lichenin, starch, xanthan and gum arabic (weak). The major cellular fatty acids are iso-15:0, iso-13:0, 16:1ω7c, 16:0. The DNA G+C content determined from genome sequence of type strain is 56.72%.

The type strain is X5P6^T (= DSMZ 117309 = HAMBI 3811) isolated from tundra soil in Malla Nature Reserve, Kilpisjärvi, Finland (69°01′N, 20°50′E). NCBI accession numbers for the 16S rRNA gene sequence and for the draft genome sequence of the type strain are OR449310 and CP132942-CP132943, respectively.

Acknowledgements

We thank Sirkka-Liisa Aakkonen, Sari Välitalo and Marika Pätsi for the help in cultivating and characterizing the strains. We thank Kristina Chew and Serena Connolly for assistance with nomenclature. This study was funded in part by the U.S. National Science Foundation (Award Number 2129351) to MMH and LJK, the Academy of Finland (decision numbers 130507 and 310776) to MKM, and the USDA National

Institute of Food and Agriculture Hatch project accession number 1012785 through the New Jersey Agricultural Experiment Station (Hatch Project NJ01160) to MMH. Illumina sequencing of select strains was done through the Community Science Program (CSP) of the US Department of Energy Joint Genomes Institute (Genomic Sequencing of Core and Pangenomes of Soil and Plant-associated Prokaryotes; PI William B. Whitman).

Author Contributions

MKM isolated and characterized the original *Tunturibacter* stains and prepared samples for DOE JGI Illumina sequencing. AM and LJK performed the MinION sequencing. AM performed the bioinformatics analysis and wrote the first draft. MKM, MMH, and LJK edited the manuscript.

Data Availability

The NCBI BioProject ID for the newly assembled *Tunturibacter* genomes is PRJNA1004338. Accession numbers for 16S rRNA genes are OR449309 - OR449318. Accession numbers for genomes are CP132926-CP132945. The rRNA operon reads from Malla Nature Reserve soil samples are available in BioProject ID PRJNA1093128.

References

Barns, S.M., Cain, E.C., Sommerville, L., and Kuske, C.R. (2007) Acidobacteria phylum sequences in uranium-contaminated subsurface sediments greatly expand the known diversity within the phylum. *Appl Environ Microbiol* **73**: 3113–3116.

Belova, S.E., Ravin, N.V., Pankratov, T.A., Rakitin, A.L., Ivanova, A.A., Beletsky, A.V., et al. (2018) Hydrolytic capabilities as a key to environmental success: Chitinolytic and cellulolytic Acidobacteria from acidic sub-arctic soils and boreal peatlands. *Front Microbiol* **9**: 2775.

Belova, S.E., Suzina, N.E., Rijpstra, W.I.C., Sinninghe Damsté, J.S., and Dedysh, S.N. (2018) *Edaphobacter lichenicola* sp. nov., a member of the family Acidobacteriaceae from lichen-dominated forested tundra. *Int J Syst Evol Microbiol* **68**: 1265–1270.

Bond-Lamberty, B. and Thomson, A. (2010) Temperature-associated increases in the global soil respiration record. *Nature* **464**: 579–582.

Campbell, B.J., Polson, S.W., Hanson, T.E., Mack, M.C., and Schuur, E.A.G. (2010) The effect of nutrient deposition on bacterial communities in Arctic tundra soil. *Environ Microbiol* **12**: 1842–1854.

Challacombe, J.F., Eichorst, S.A., Hauser, L., Land, M., Xie, G., and Kuske, C.R. (2011) Biological consequences of ancient gene acquisition and duplication in the large genome of *Candidatus Solibacter usitatus* Ellin6076. *PLOS ONE* **6**: e24882.

Chesson, P. (2000) Mechanisms of maintenance of species diversity. *Annual Review of Ecology and Systematics* **31**: 343–366.

Chesson, P. and Huntly, N. (1997) The roles of harsh and fluctuating conditions in the dynamics of ecological communities. *The American Naturalist* **150**: 519–553.

Chu, H., Fierer, N., Lauber, C.L., Caporaso, J.G., Knight, R., and Grogan, P. (2010) Soil bacterial diversity in the Arctic is not fundamentally different from that found in other biomes. *Environ Microbiol* **12**: 2998–3006.

Crits-Christoph, A., Diamond, S., Al-Shayeb, B., Valentin-Alvarado, L., and Banfield, J.F. (2022) A widely distributed genus of soil Acidobacteria genomically enriched in biosynthetic gene clusters. *ISME COMMUN* **2**: 1–8.

Darling, A.C.E., Mau, B., Blattner, F.R., and Perna, N.T. (2004) Mauve: Multiple alignment of conserved genomic sequence with rearrangements. *Genome Res* **14**: 1394–1403.

Davis, K.E.R., Joseph, S.J., and Janssen, P.H. (2005) Effects of growth medium, inoculum size, and incubation time on culturability and isolation of soil bacteria. *Appl Environ Microbiol* **71**: 826–834.

Dedysh, S.N., Ivanova, A.A., Begmatov, Sh.A., Beletsky, A.V., Rakitin, A.L., Mardanov, A.V., et al. (2022) Acidobacteria in fens: Phylogenetic diversity and genome analysis of the key representatives. *Microbiology* **91**: 662–670.

Dedysh, S.N. and Yilmaz, P. (2018) Refining the taxonomic structure of the phylum Acidobacteria. *Int J Syst Evol Microbiol* **68**: 3796–3806.

Dhakal, R., Bajpai, V.K., and Baek, K.-H. (2012) Production of gaba (γ – Aminobutyric acid) by microorganisms: a review. *Braz J Microbiol* **43**: 1230–1241.

Diamond, S., Andeer, P.F., Li, Z., Crits-Christoph, A., Burstein, D., Anantharaman, K., et al. (2019) Mediterranean grassland soil C–N compound turnover is dependent on rainfall and depth, and is mediated by genomically divergent microorganisms. *Nat Microbiol* **4**: 1356–1367.

Eddy, S. R. (2011) Accelerated Profile HMM Searches. *PLoS Comput. Biol.* **7:** e1002195

Edgar, R.C. (2021) MUSCLE v5 enables improved estimates of phylogenetic tree confidence by ensemble bootstrapping. 2021.06.20.449169.

Eichorst, S.A., Breznak, J.A., and Schmidt, T.M. (2007) Isolation and characterization of soil bacteria that define *Terriglobus* gen. nov., in the phylum Acidobacteria. *Appl Environ Microbiol* **73**: 2708–2717.

Eichorst, S.A., Trojan, D., Roux, S., Herbold, C., Rattei, T., and Woebken, D. (2018) Genomic insights into the Acidobacteria reveal strategies for their success in terrestrial environments. *Environmental Microbiology* **20**: 1041–1063.

Emms, D.M. and Kelly, S. (2019) OrthoFinder: phylogenetic orthology inference for comparative genomics. *Genome Biology* **20**: 238.

Eren, A.M., Kiefl, E., Shaiber, A., Veseli, I., Miller, S.E., Schechter, M.S., et al. (2021) Community-led, integrated, reproducible multi-omics with anvi'o. *Nat Microbiol* **6**: 3–6.

744 Eskelinen, A., Stark, S., and Männistö, M. (2009) Links between plant community composition, soil organic matter quality and microbial communities in contrasting tundra habitats. *Oecologia* **161**: 113–123.
747 Fry, E.L., Ashworth, D., Allen, K.A.J., Chardon, N.I., Rixen, C., Björkman, M.P., et al. (2023) Vegetation type, not the legacy of warming, modifies the response of microbial functional genes and greenhouse gas fluxes to drought in oro-arctic
750 and alpine regions. *FEMS Microbiology Ecology* **99:** fiad145.
Gadkari, P.S., McGuinness, L.R., Männistö, M.K., Kerkhof, L.J., and Häggblom, M.M. (2020) Arctic tundra soil bacterial communities active at subzero temperatures
753 detected by stable isotope probing. *FEMS Microbiology Ecology* **96**: fiz192.
Schmartz, G.P., Hartung, A., Hirsch, P., Kern, F., Fehlmann, T., Müller, R., Keller, A. (2021) PLSDB: advancing a comprehensive database of bacterial plasmids.
756 *Nucleic Acids Res* **50**: D273–D278.
German Collection of Microorganisms and Cell Cultures GmbH: Polar Lipids.
German Collection of Microorganisms and Cell Cultures GmbH: Respiratory Quinones.
759 Ghoul, M. and Mitri, S. (2016) The ecology and evolution of microbial competition. *Trends in Microbiology* **24**: 833–845.
Göker, M. (2023) Filling the gaps: missing taxon names at the ranks of class, order and
762 family. *International Journal of Systematic and Evolutionary Microbiology* **72**: 005638.
Graham, D.E., Wallenstein, M.D., Vishnivetskaya, T.A., Waldrop, M.P., Phelps, T.J.,
765 Pfiffner, S.M., et al. (2012) Microbes in thawing permafrost: the unknown variable in the climate change equation. *ISME J* **6**: 709–712.
Gurevich, A., Saveliev, V., Vyahhi, N., and Tesler, G. (2013) QUAST: quality
768 assessment tool for genome assemblies. *Bioinformatics* **29**: 1072–1075.
Hugelius, G., Strauss, J., Zubrzycki, S., Harden, J.W., Schuur, E. a. G., Ping, C.-L., et al. (2014) Estimated stocks of circumpolar permafrost carbon with quantified
771 uncertainty ranges and identified data gaps. *Biogeosciences* **11**: 6573–6593.
Ivanova, A.A., Zhelezova, A.D., Chernov, T.I., and Dedysh, S.N. (2020) Linking ecology and systematics of acidobacteria: Distinct habitat preferences of the
774 Acidobacteriia and Blastocatellia in tundra soils. *PLOS ONE* **15**: e0230157.
Janssen, P.H. (2006) Identifying the dominant soil bacterial taxa in libraries of 16S rRNA and 16S rRNA genes. *Appl Environ Microbiol* **72**: 1719–1728.
777 Jonasson, S., Michelsen, A., and Schmidt, I.K. (1999) Coupling of nutrient cycling and carbon dynamics in the Arctic, integration of soil microbial and plant processes. *Appl Soil Ecol*. **11:** 135–46.
780 Jones, R.T., Robeson, M.S., Lauber, C.L., Hamady, M., Knight, R., and Fierer, N. (2009) A comprehensive survey of soil acidobacterial diversity using pyrosequencing and clone library analyses. *ISME J* **3**: 442–453.
783 Kalam, S., Basu, A., Ahmad, I., Sayyed, R.Z., El-Enshasy, H.A., Dailin, D.J., and Suriani, N.L. (2020) Recent understanding of soil Acidobacteria and their ecological significance: A critical review. *Frontiers in Microbiology* **11**: 580024.
786 Kielak, A.M., Barreto, C.C., Kowalchuk, G.A., van Veen, J.A., and Kuramae, E.E. (2016) The ecology of Acidobacteria: Moving beyond genes and genomes. *Frontiers in Microbiology* **7**: 744.

Kim, H.M., Jung, J.Y., Yergeau, E., Hwang, C.Y., Hinzman, L., Nam, S., et al. (2014) Bacterial community structure and soil properties of a subarctic tundra soil in Council, Alaska. *FEMS Microbiology Ecology* **89**: 465–475.

Kishimoto, N., Kosako, Y., and Tano, T. (1991) *Acidobacterium capsulatum* gen. nov., sp. nov.: An acidophilic chemoorganotrophic bacterium containing menaquinone from acidic mineral environment. *Current Microbiology* **22**: 1–7.

Koch, I.H., Gich, F., Dunfield, P.F., and Overmann, J. (2008) Edaphobacter modestus gen. nov., sp. nov., and Edaphobacter aggregans sp. nov., acidobacteria isolated from alpine and forest soils. *Int J Syst Evol Microbiol* **58**: 1114–1122.

Kolmogorov, M., Yuan, J., Lin, Y., and Pevzner, P.A. (2019) Assembly of long, error-prone reads using repeat graphs. *Nat Biotechnol* **37**: 540–546.

Koven, C.D., Ringeval, B., Friedlingstein, P., Ciais, P., Cadule, P., Khvorostyanov, D., et al. (2011) Permafrost carbon-climate feedbacks accelerate global warming. *Proceedings of the National Academy of Sciences* **108**: 14769–14774.

Lane, D.J. (1991) 16S/23S rRNA sequencing. In Nucleic Acid Techniques in Bacterial Systematics, pp. 115–175. Edited by E. Stackebrandt & M. Goodfellow. Chichester: Wiley.

Lee, M.D. (2019) GtoTree: a user-friendly workflow for phylogenomics. *Bioinformatics* **35**: 4162–4164.

Lennon, J.T., Aanderud, Z.T., Lehmkuhl, B.K., and Schoolmaster Jr., D.R. (2012) Mapping the niche space of soil microorganisms using taxonomy and traits. *Ecology* **93**: 1867–1879.

Letunic, I. and Bork, P. (2021) Interactive Tree Of Life (iTOL) v5: an online tool for phylogenetic tree display and annotation. *Nucleic Acids Research* **49**: W293–W296.

Lin, Y., Yuan, J., Kolmogorov, M., Shen, M.W., Chaisson, M., and Pevzner, P.A. (2016) Assembly of long error-prone reads using de Bruijn graphs. *Proceedings of the National Academy of Sciences* **113**: E8396–E8405.

Loya, W.M. and Grogan, P. (2004) Carbon conundrum on the tundra. *Nature* **431**: 406–408.

Männistö, M.K., Ahonen, S.H.K., Ganzert, L., Tiirola, M., Stark, S., and Häggblom, M.M. (2024) Bacterial and fungal communities in sub-Arctic tundra heaths are shaped by contrasting snow accumulation and nutrient availability. *FEMS Microbiology Ecology* **100:** fiae036.

Männistö, M., Vuosku, J., Stark, S., Saravesi, K., Suokas, M., Markkola, A., et al. (2018) Bacterial and fungal communities in boreal forest soil are insensitive to changes in snow cover conditions. *FEMS Microbiology Ecology* **94**: fiy123.

Männistö, M.K., Kurhela, E., Tiirola, M., and Häggblom, M.M. (2013) Acidobacteria dominate the active bacterial communities of Arctic tundra with widely divergent winter-time snow accumulation and soil temperatures. *FEMS Microbiol Ecol* **84**: 47–59.

Männistö, M.K., Rawat, S., Starovoytov, V., and Häggblom, M.M. (2012) *Granulicella arctica* sp. nov., *Granulicella mallensis* sp. nov., *Granulicella tundricola* sp. nov. and *Granulicella sapmiensis* sp. nov., novel acidobacteria from tundra soil. *Int J Syst Evol Microbiol* **62**: 2097–2106.

Männistö, M.K., Rawat, S., Starovoytov, V., and Häggblom, M.M. (2011) *Terriglobus saanensis* sp. nov., an acidobacterium isolated from tundra soil. *Int J Syst Evol Microbiol* **61**: 1823–1828.

Männistö, M.K., Tiirola, M., and Häggblom, M.M. (2007) Bacterial communities in Arctic fjelds of Finnish Lapland are stable but highly pH-dependent. *FEMS Microbiology Ecology* **59**: 452–465.

Männistö, M.K., Tiirola, M., and Häggblom, M.M. (2009) Effect of freeze-thaw cycles on bacterial communities of arctic tundra soil. *Microb Ecol* **58**: 621–631.

McMahon, S.K., Wallenstein, M.D., and Schimel, J.P. (2011) A cross-seasonal comparison of active and total bacterial community composition in Arctic tundra soil using bromodeoxyuridine labeling. *Soil Biology and Biochemistry* **43**: 287–295.

Miller, S.E., Colman, A.S., and Waldbauer, J.R. (2023) Metaproteomics reveals functional partitioning and vegetational variation among permafrost-affected Arctic soil bacterial communities. *mSystems* **8**: e01238-22.

Natali, S.M., Schuur, E.A.G., Webb, E.E., Pries, C.E.H., and Crummer, K.G. (2014) Permafrost degradation stimulates carbon loss from experimentally warmed tundra. *Ecology* **95**: 602–608.

Nikrad, M.P., Kerkhof, L.J., and Häggblom, M.M. (2016) The subzero microbiome: microbial activity in frozen and thawing soils. *FEMS Microbiol Ecol* **92**: fiw081.

Oechel, W.C., Vourlitis, G., and Hastings, S.J. (1997) Cold season CO_2 emission from Arctic soils. *Global Biogeochemical Cycles* **11**: 163–172.

Ondov, B.D., Treangen, T.J., Melsted, P. et al. (2016) Mash: fast genome and metagenome distance estimation using MinHash. *Genome Biol* **17**, 132.

Pankratov, T.A. and Dedysh, S.N. (2010) *Granulicella paludicola* gen. nov., sp. nov., *Granulicella pectinivorans* sp. nov., *Granulicella aggregans* sp. nov. and *Granulicella rosea* sp. nov., acidophilic, polymer-degrading acidobacteria from *Sphagnum* peat bogs. *Int J Syst Evol Microbiol* **60**: 2951–2959.

Parks, D.H., Chuvochina, M., Rinke, C., Mussig, A.J., Chaumeil, P.-A., and Hugenholtz, P. (2022) GTDB: an ongoing census of bacterial and archaeal diversity through a phylogenetically consistent, rank normalized and complete genome-based taxonomy. *Nucleic Acids Research* **50**: D785–D794.

Parks, D.H., Imelfort, M., Skennerton, C.T., Hugenholtz, P., and Tyson, G.W. (2015) CheckM: assessing the quality of microbial genomes recovered from isolates, single cells, and metagenomes. *Genome Res* **25**: 1043–1055.

Parsek, M.R., Val D.L., Hanzelka, B.L., Cronan, J.E., and Greenberg E.P. (1998) Acyl homoserine-lactone quorum-sensing signal generation. *Proc Natl Acad Sci U S A* **96**: 4360–4365.

Parsley, L.C., Linneman, J., Goode, A.M., Becklund, K., George, I., Goodman, R.M., et al. (2011) Polyketide synthase pathways identified from a metagenomic library are derived from soil Acidobacteria. *FEMS Microbiol Ecol* **78**: 176–187.

Pessi, I.S., Viitamäki, S., Virkkala, A.-M., Eronen-Rasimus, E., Delmont, T.O., Marushchak, M.E., et al. (2022) In-depth characterization of denitrifier communities across different soil ecosystems in the tundra. *Environmental Microbiome* **17**: 30.

879 Podar, M., Turner, J., Burdick, L.H., and Pelletier, D.A. (2019) Complete Genome Sequence of *Terriglobus albidus* Strain ORNL, an Acidobacterium Isolated from the *Populus deltoides* Rhizosphere. *Microbiology Resource Announcements* **8**: 882 e01065-19.

Poppeliers, S.W.M., Hefting, M., Dorrepaal, E., and Weedon, J.T. (2022) Functional microbial ecology in arctic soils: the need for a year-round perspective. *FEMS* 885 *Microbiol Ecol* **98**: fiac134.

Price, M.N., Dehal, P.S., and Arkin, A.P. (2010) FastTree 2 – Approximately Maximum-Likelihood Trees for Large Alignments. *PLOS ONE* **5**: e9490.

888 Pritchard, L., Glover, R.H., Humphris, S., Elphinstone, J.G., and Toth, I.K. (2015) Genomics and taxonomy in diagnostics for food security: soft-rotting enterobacterial plant pathogens. *Anal Methods* **8**: 12–24.

891 Rawat, S.R., Männistö, M.K., Starovoytov, V., Goodwin, L., Nolan, M., Hauser, L., et al. (2014) Complete genome sequence of *Granulicella tundricola* type strain MP5ACTX9(T), an Acidobacteria from tundra soil. *Stand Genomic Sci* **9**: 449–894 461.

Rawat, S.R., Männistö, M.K., Starovoytov, V., Goodwin, L., Nolan, M., Hauser, L., et al. (2012) Complete genome sequence of *Terriglobus saanensis* type strain 897 SP1PR4(T), an Acidobacteria from tundra soil. *Stand Genomic Sci* **7**: 59–69.

Rawat, S.R., Männistö, M.K., Starovoytov, V., Goodwin, L., Nolan, M., Hauser, L.J., et al. (2013) Complete genome sequence of *Granulicella mallensis* type strain 900 MP5ACTX8T, an acidobacterium from tundra soil. *Stand Genomic Sci* **9**: 71–82.

Riaz, K., Elmerich, C., Moreira, D., Raffoux, A., Dessaux, Y., and Faure, D. (2008) A metagenomic analysis of soil bacteria extends the diversity of quorum-quenching 903 lactonases. *Environ Microbiol.* **10**: 560-70.

Ruhl, I.A., Sheremet, A., Furgason, C.C., Krause, S., Bowers, R.M., Jarett, J.K., et al. (2022) GAL08, an uncultivated group of Acidobacteria, is a dominant bacterial 906 clade in a neutral hot spring. *Frontiers in Microbiology* **12**: 787651.

Seeman, Torsten (2014) Prokka: rapid prokaryotic genome annotation. *Bioinformatics* **15**: 2068-9

909 Schuur, E.A.G., Bockheim, J., Canadell, J.G., Euskirchen, E., Field, C.B., Goryachkin, S.V., et al. (2008) Vulnerability of permafrost carbon to climate change: Implications for the global carbon cycle. *BioScience* **58**: 701–714.

912 Shaiber, A., Willis, A.D., Delmont, T.O., Roux, S., Chen, L.-X., Schmid, A.C., et al. (2020) Functional and genetic markers of niche partitioning among enigmatic members of the human oral microbiome. *Genome Biology* **21**: 292.

915 Shimoyama, Y. (2022) pyGenomeViz: A genome visualization python package for comparative genomics.

Stark, S., Kytöviita, M.-M. (2006) Simulated grazer effects on microbial respiration in a 918 subarctic meadow: Implications for nutrient competition between plants and soil microorganisms. *Appl Soil Ecol*. **31:** 20–31.

Stark, S., Kumar, M., Myrsky, E., Vuorinen, J., Kantola, A.M., Telkki, V.-V., et al. (2023) 921 Decreased soil microbial nitrogen under vegetation 'shrubification' in the subarctic forest–tundra ecotone: The potential role of increasing nutrient competition between plants and soil microorganisms. *Ecosystems* **26:** 1504–924 1523

Taş, N., Prestat, E., Wang, S., Wu, Y., Ulrich, C., Kneafsey, T., et al. (2018) Landscape topography structures the soil microbiome in arctic polygonal tundra. *Nat Commun* **9**: 777.

Tveit, A.T., Urich, T., and Svenning, M.M. (2014) Metatranscriptomic analysis of arctic peat soil microbiota. *Applied and Environmental Microbiology* **80**: 5761–5772.

Vaser, R. and Šikić, M. (2021) Time- and memory-efficient genome assembly with Raven. *Nat Comput Sci* **1**: 332–336.

Viitamäki, S., Pessi, I.S., Virkkala, A.-M., Niittynen, P., Kemppinen, J., Eronen-Rasimus, E., et al. (2022) The activity and functions of soil microbial communities in the Finnish sub-Arctic vary across vegetation types. *FEMS Microbiol Ecol* **98**: fiac079.

Voříšková, J., Elberling, B., and Priemé, A. (2019) Fast response of fungal and prokaryotic communities to climate change manipulation in two contrasting tundra soils. *Environmental Microbiome* **14**: 6.

Wang, J., Chen, M.-H., Lv, Y.-Y., Jiang, Y.-W., and Qiu, L.-H. (2016) *Edaphobacter dinghuensis* sp. nov., an acidobacterium isolated from lower subtropical forest soil. *Int J Syst Evol Microbiol* **66**: 276–282.

Ward, N.L., Challacombe, J.F., Janssen, P.H., Henrissat, B., Coutinho, P.M., Wu, M., et al. (2009) Three genomes from the phylum Acidobacteria provide insight into the lifestyles of these microorganisms in soils. *Appl Environ Microbiol* **75**: 2046–2056.

Weintraub, M.N. and Schimel, J.P. (2003) Interactions between carbon and nitrogen mineralization and soil organic matter chemistry in arctic tundra soils. *Ecosystems* **6**: 129–143.

Welker, J.M., Fahnestock, J.T., and Jones, M.H. (2000) Annual CO_2 flux in dry and moist arctic tundra: Field responses to increases in summer temperatures and winter snow depth. *Climatic Change* **44**: 139–150.

Wick, R.R. and Holt, K.E. (2019) Benchmarking of long-read assemblers for prokaryote whole genome sequencing. *F1000Res* **8**: 2138.

Wick, R.R. and Holt, K.E. (2022) Polypolish: Short-read polishing of long-read bacterial genome assemblies. *PLOS Computational Biology* **18**: e1009802.

Wick, R.R., Judd, L.M., Cerdeira, L.T., Hawkey, J., Méric, G., Vezina, B., et al. (2021) Trycycler: consensus long-read assemblies for bacterial genomes. *Genome Biology* **22**: 266.

Yoon, S. H., Ha, S. M., Kwon, S., Lim, J., Kim, Y., Seo, H. and Chun, J. (2017) Introducing EzBioCloud: A taxonomically united database of 16S rRNA and whole genome assemblies. *Int J Syst Evol Microbiol.* **67:**1613-1617

Zhang H., Yohe T., Huang L., Entwistle S., Wu P., Yang Z., Busk P.K., Xu Y. and Yin Y. (2018) dbCAN2: a meta server for automated carbohydrate-active enzyme annotation. *Nucleic Acids Res*. **46**(W1):W95-W101.

Zhang, Q.-M., Fu, J.-C., Chen, Z.-Q., and Qiu, L.-H. (2022) *Paracidobacterium acidisoli* gen. nov., sp. nov. and *Alloacidobacterium dinghuense* gen. nov., sp. nov., two acidobacteria isolated from forest soil, and reclassification of *Acidobacterium ailaaui* and *Acidipila dinghuensis* as *Pseudacidobacterium ailaaui* gen. nov., comb. nov. and *Silvibacterium dinghuense* comb. nov. *Int J Syst Evol Microbiol* **72**: :005415.

Zinger, L., Shahnavaz, B., Baptist, F., Geremia, R.A., and Choler, P. (2009) Microbial diversity in alpine tundra soils correlates with snow cover dynamics. *ISME J* **3**: 850–859.

FIGURE LEGENDS

Figure 1. A) Single copy gene phylogeny of *Terriglobia* genomes, B) Sub-tree of the phylogenetic placement of the new *Tunturibacter* genus with more closely related genera. Accession numbers for genomes available from NCBI are listed in Table S3.

Figure 2. Pangenome analysis of the *Terriglobia* in the *Acidobacteriota*. Comparison of gene clusters between the 13 assembled tundra soil isolates and known *Terriglobia*. Each row designating an *Acidobacteriota* strain starts with information on the presence of gene clusters (gene clusters are marked by the darker-colored regions within the row). This is followed by the red/maroon columns indicating levels of: genome total length, number of genes per kbp, singleton gene clusters, and number of gene clusters. These columns are followed by the ANI data from the pangenome analysis, and the grouping of the *Acidobacteriota* based on gene cluster frequency (right-hand tree). Under the gene cluster presence rows are rows indicating COG20, KEGG, and Kofam annotations, SCG clusters, and number of genes and contributing genomes in the gene cluster.

Figure 3. Circularized Anvio pangenome of the *Terriglobia*.

Figure 4. Genome comparisons at various taxonomic levels. A) Comparison of 4 SD1 *Acidobacteriota* including *Tunturibacter lichenicola*. B) Comparison of the 4 species within the *Tunturibacter* (each species represents the type strain). C) Comparison of 4 strains within the *Tunturibacter empetritectus*. Genome comparisons were viewed via PGV-Mummer. Black horizontal lines indicate the span of the genome being compared, green lines connect homologous regions between the genomes in the same orientation (normal link), brown lines connect homologous regions of between the genomes in reverse orientation (inverted link). The shade of the green and brown indicate percent homology (bottom right legend, dark color means higher percent homology).

Figure 5. *Terriglobia* community in soils of windswept (K1, K3, K6, K8) and snow-accumulating (T2, T5, T6, T7) tundra heath plots of Mt. Pikku Malla. rRNA operon reads from the *Acidobacteriota* represent 4.2-18.4% of the total bacterial reads.

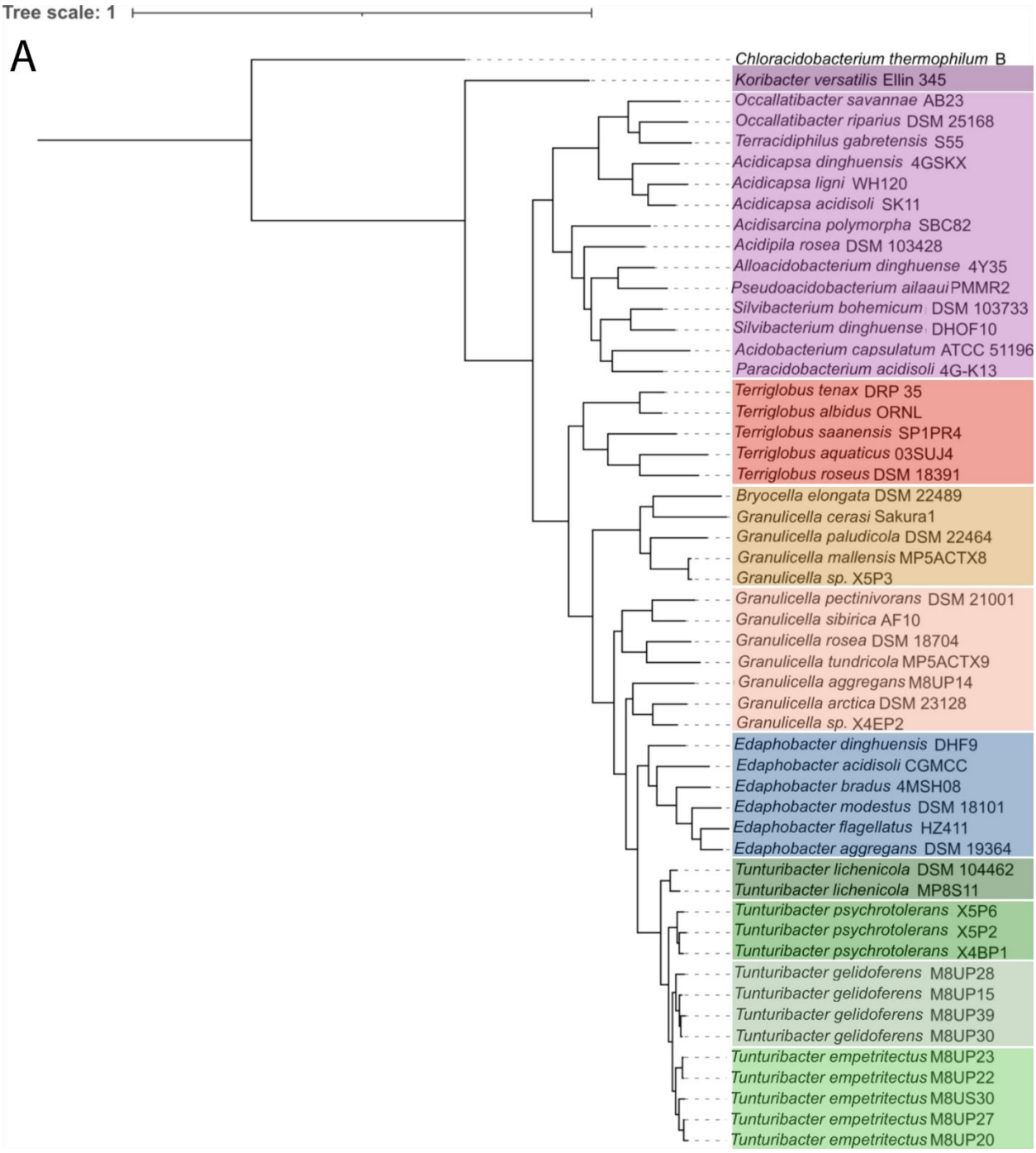
Tree scale: 1
A
Chloracidobacterium thermophilum B
Koribacter versatilis Ellin 345
Occallatibacter savannae AB23
Occallatibacter riparius DSM 25168
Terracidiphilus gabretensis S55
Acidicapsa dinghuensis 4GSKX
Acidicapsa ligni WH120
Acidicapsa acidisoli SK11
Acidisarcina polymorpha SBC82
Acidipila rosea DSM 103428
Alloacidobacterium dinghuense 4Y35
Pseudoacidobacterium ailaaui PMMR2
Silvibacterium bohemicum DSM 103733
Silvibacterium dinghuense DHOF10
Acidobacterium capsulatum ATCC 51196
Paracidobacterium acidisoli 4G-K13
Terriglobus tenax DRP 35
Terriglobus albidus ORNL
Terriglobus saanensis SP1PR4
Terriglobus aquaticus 03SUJ4
Terriglobus roseus DSM 18391
Bryocella elongata DSM 22489
Granulicella cerasi Sakura1
Granulicella paludicola DSM 22464
Granulicella mallensis MP5ACTX8
Granulicella sp. X5P3
Granulicella pectinivorans DSM 21001
Granulicella sibirica AF10
Granulicella rosea DSM 18704
Granulicella tundricola MP5ACTX9
Granulicella aggregans M8UP14
Granulicella arctica DSM 23128
Granulicella sp. X4EP2
Edaphobacter dinghuensis DHF9
Edaphobacter acidisoli CGMCC
Edaphobacter bradus 4MSH08
Edaphobacter modestus DSM 18101
Edaphobacter flagellatus HZ411
Edaphobacter aggregans DSM 19364
Tunturibacter lichenicola DSM 104462
Tunturibacter lichenicola MP8S11
Tunturibacter psychrotolerans X5P6
Tunturibacter psychrotolerans X5P2
Tunturibacter psychrotolerans X4BP1
Tunturibacter gelidoferens M8UP28
Tunturibacter gelidoferens M8UP15
Tunturibacter gelidoferens M8UP39
Tunturibacter gelidoferens M8UP30
Tunturibacter empetritectus M8UP23
Tunturibacter empetritectus M8UP22
Tunturibacter empetritectus M8US30
Tunturibacter empetritectus M8UP27
Tunturibacter empetritectus M8UP20

1011

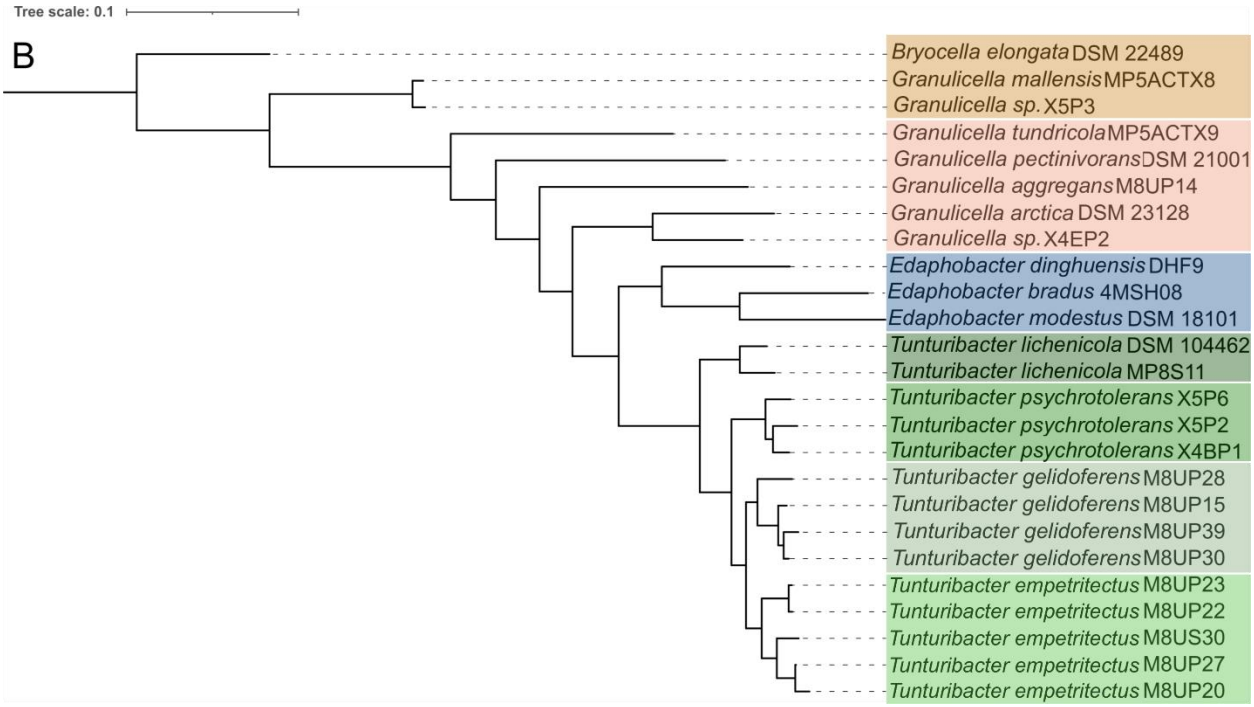
Tree scale: 0.1
B
Bryocella elongata DSM 22489
Granulicella mallensis MP5ACTX8
Granulicella sp. X5P3
Granulicella tundricola MP5ACTX9
Granulicella pectinivorans DSM 21001
Granulicella aggregans M8UP14
Granulicella arctica DSM 23128
Granulicella sp. X4EP2
Edaphobacter dinghuensis DHF9
Edaphobacter bradus 4MSH08
Edaphobacter modestus DSM 18101
Tunturibacter lichenicola DSM 104462
Tunturibacter lichenicola MP8S11
Tunturibacter psychrotolerans X5P6
Tunturibacter psychrotolerans X5P2
Tunturibacter psychrotolerans X4BP1
Tunturibacter gelidoferens M8UP28
Tunturibacter gelidoferens M8UP15
Tunturibacter gelidoferens M8UP39
Tunturibacter gelidoferens M8UP30
Tunturibacter empetritectus M8UP23
Tunturibacter empetritectus M8UP22
Tunturibacter empetritectus M8US30
Tunturibacter empetritectus M8UP27
Tunturibacter empetritectus M8UP20

1014

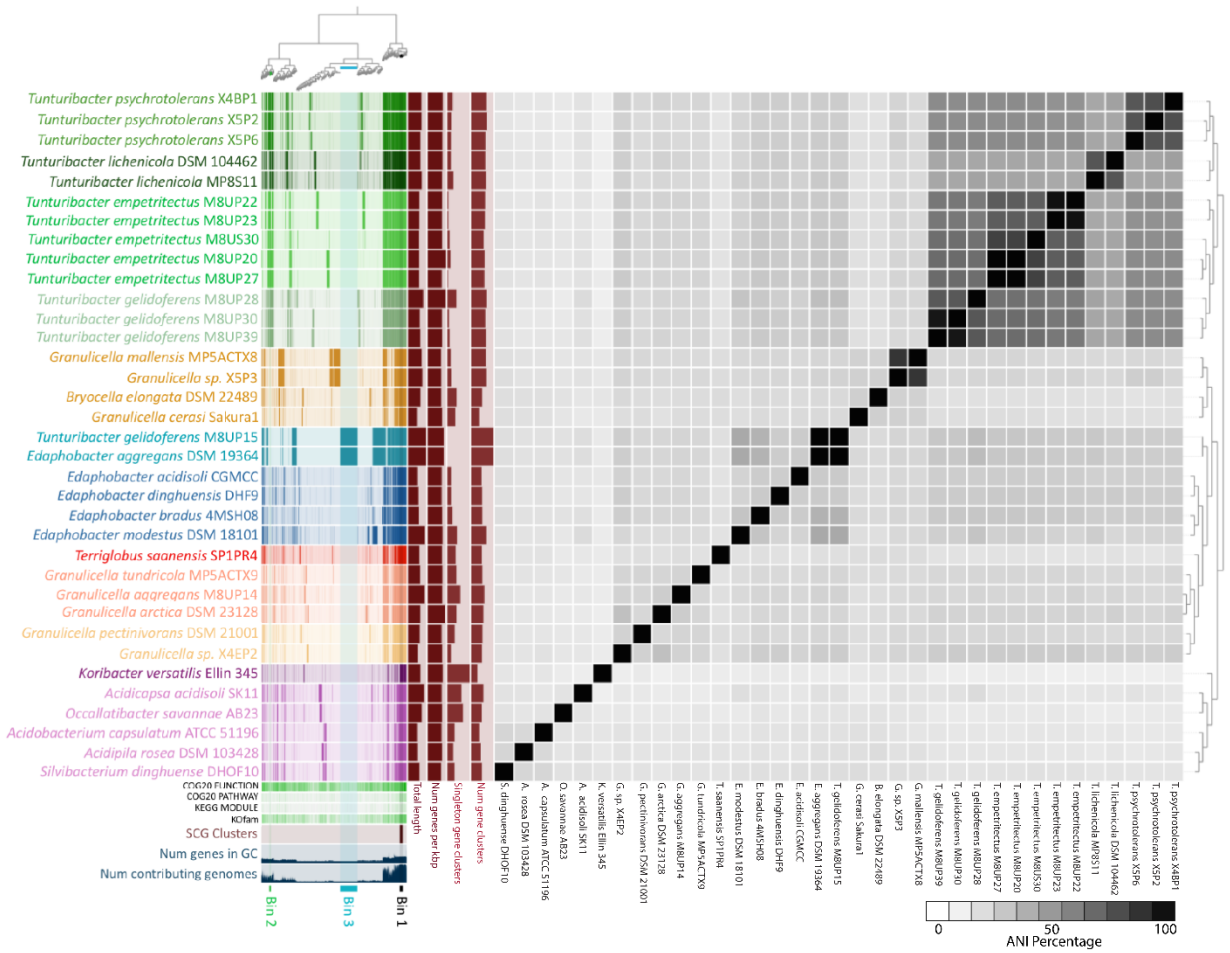
Tunturibacter psychrotolerans X4BP1
Tunturibacter psychrotolerans X5P2
Tunturibacter psychrotolerans X5P6
Tunturibacter lichenicola DSM 104462
Tunturibacter lichenicola MP8S11
Tunturibacter empetritectus M8UP22
Tunturibacter empetritectus M8UP23
Tunturibacter empetritectus M8US30
Tunturibacter empetritectus M8UP20
Tunturibacter empetritectus M8UP27
Tunturibacter gelidoferens M8UP28
Tunturibacter gelidoferens M8UP30
Tunturibacter gelidoferens M8UP39
Granulicella mallensis MP5ACTX8
Granulicella sp. X5P3
Bryocella elongata DSM 22489
Granulicella cerasi Sakura1
Tunturibacter gelidoferens M8UP15
Edaphobacter aggregans DSM 19364
Edaphobacter acidisoli CGMCC
Edaphobacter dinghuensis DHF9
Edaphobacter bradus 4MSH08
Edaphobacter modestus DSM 18101
Terriglobus saanensis SP1PR4
Granulicella tundricola MP5ACTX9
Granulicella aggregans M8UP14
Granulicella arctica DSM 23128
Granulicella pectinivorans DSM 21001
Granulicella sp. X4EP2
Koribacter versatilis Ellin 345
Acidicapsa acidisoli SK11
Occallatibacter savannae AB23
Acidobacterium capsulatum ATCC 51196
Acidipila rosea DSM 103428
Silvibacterium dinghuense DHOF10
COG20 FUNCTION
COG20 PATHWAY
KEGG MODULE
KOfam
SCG Clusters
Num genes in GC
Num contributing genomes
Bin 2
Bin 3
Bin 1
Total length
Num genes per kbp
Singleton gene clusters
Num gene clusters
S. dinghuense DHOF10
A. rosea DSM 103428
A. capsulatum ATCC 51196
O. savannae AB23
A. acidisoli SK11
K. versatilis Ellin 345
G. sp. X4EP2
G. pectinivorans DSM 21001
G. arctica DSM 23128
G. aggregans M8UP14
G. tundricola MP5ACTX9
T. saanensis SP1PR4
E. modestus DSM 18101
E. bradus 4MSH08
E. dinghuensis DHF9
E. acidisoli CGMCC
E. aggregans DSM 19364
T. gelidoferens M8UP15
G. cerasi Sakura1
B. elongata DSM 22489
G. sp. X5P3
G. mallensis MP5ACTX8
T. gelidoferens M8UP39
T. gelidoferens M8UP30
T. gelidoferens M8UP28
T. empetritectus M8UP27
T. empetritectus M8UP20
T. empetritectus M8US30
T. empetritectus M8UP23
T. empetritectus M8UP22
T. lichenicola MP8S11
T. lichenicola DSM 104462
T. psychrotolerans X5P6
T. psychrotolerans X5P2
T. psychrotolerans X4BP1
0
50
100
ANI Percentage

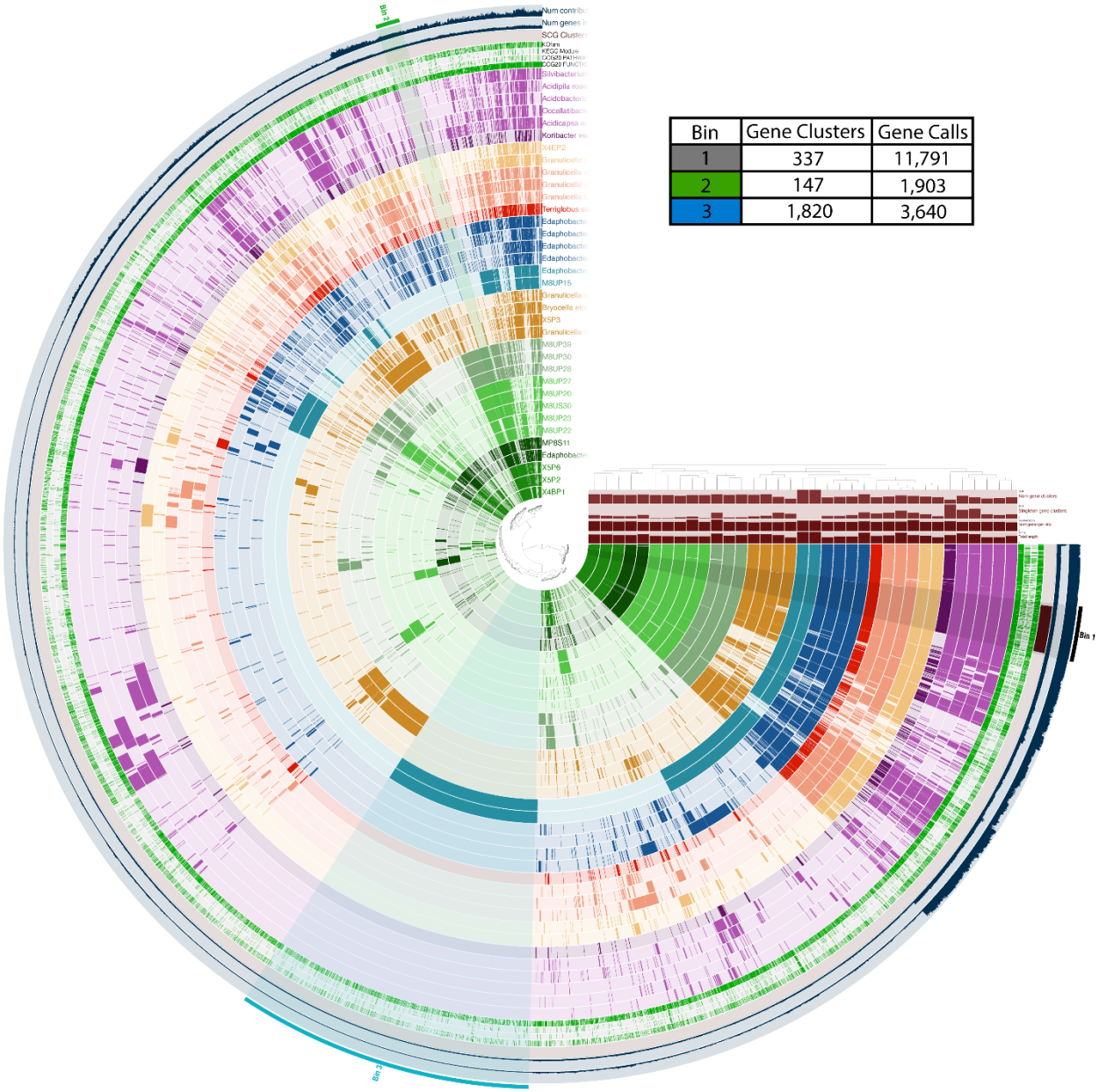

Bin	Gene Clusters	Gene Calls
1	337	11,791
2	147	1,903
3	1,820	3,640

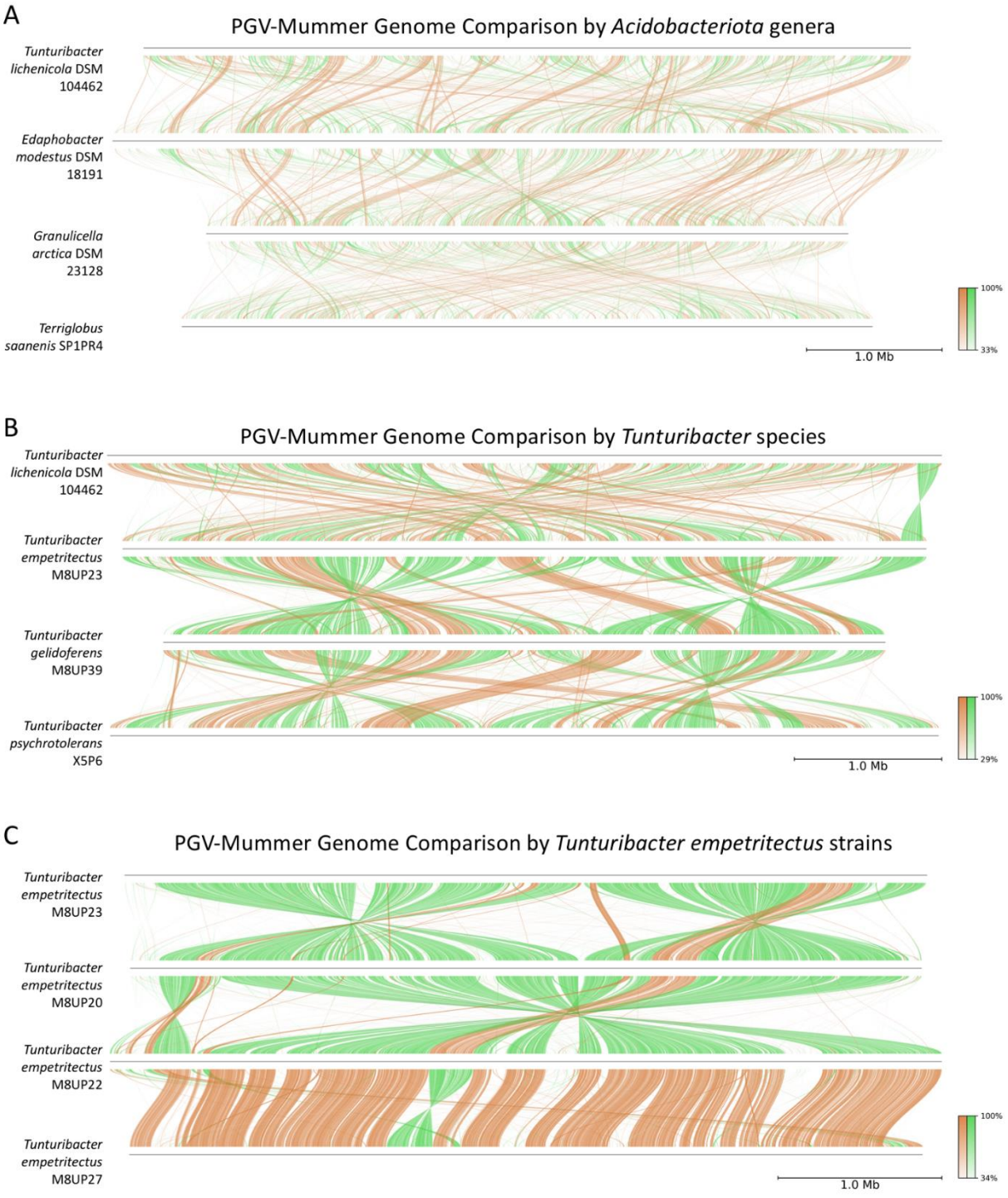
A
PGV-Mummer Genome Comparison by *Acidobacteriota* genera
Tunturibacter lichenicola DSM 104462
Edaphobacter modestus DSM 18191
Granulicella arctica DSM 23128
Terriglobus saanenis SP1PR4
100%
33%
1.0 Mb
B
PGV-Mummer Genome Comparison by *Tunturibacter* species
Tunturibacter lichenicola DSM 104462
Tunturibacter empetritectus M8UP23
Tunturibacter gelidoferens M8UP39
Tunturibacter psychrotolerans X5P6
100%
29%
1.0 Mb
C
PGV-Mummer Genome Comparison by *Tunturibacter empetritectus* strains
Tunturibacter empetritectus M8UP23
Tunturibacter empetritectus M8UP20
Tunturibacter empetritectus M8UP22
Tunturibacter empetritectus M8UP27
100%
34%
1.0 Mb

1020

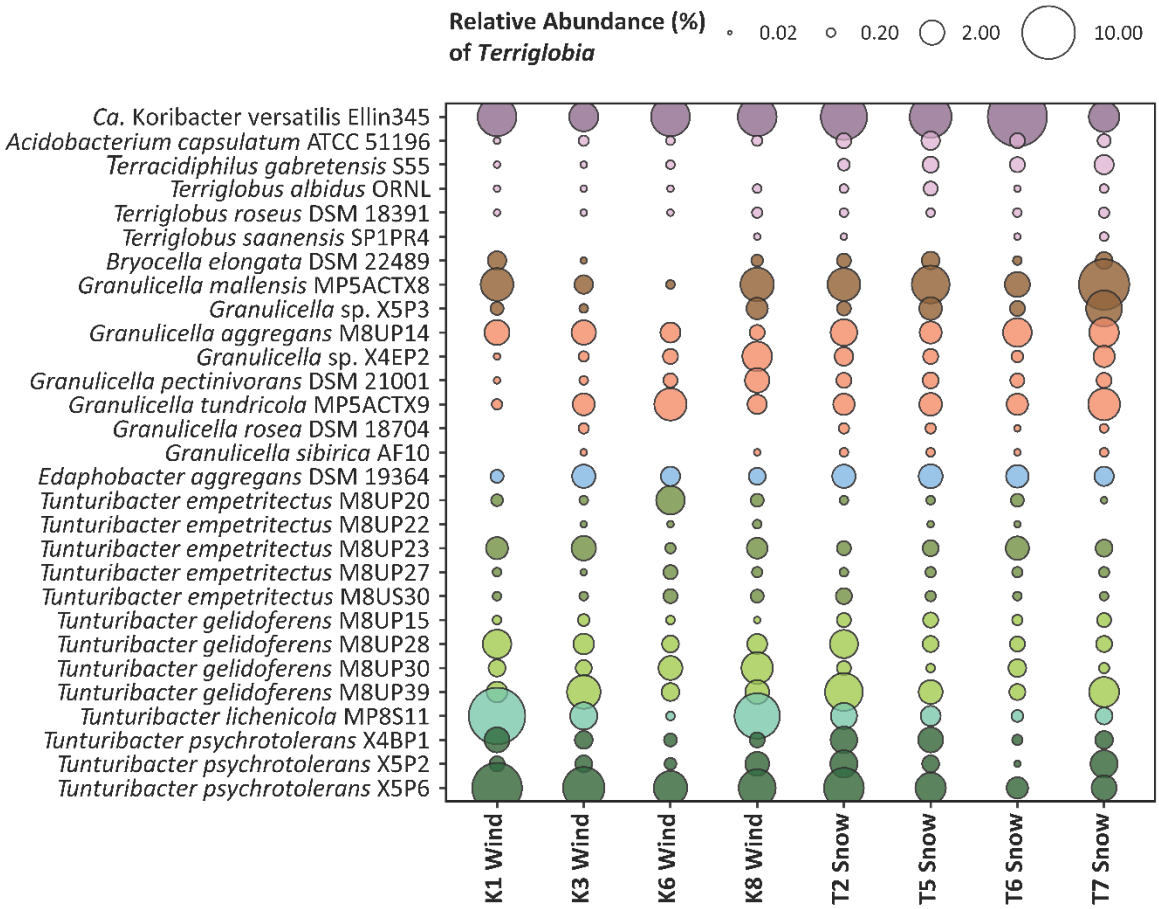
Relative Abundance (%)
of Terriglobia
0.02
0.20
2.00
10.00
Ca. Koribacter versatilis Ellin345
Acidobacterium capsulatum ATCC 51196
Terracidiphilus gabretensis S55
Terriglobus albidus ORNL
Terriglobus roseus DSM 18391
Terriglobus saanensis SP1PR4
Bryocella elongata DSM 22489
Granulicella mallensis MP5ACTX8
Granulicella sp. X5P3
Granulicella aggregans M8UP14
Granulicella sp. X4EP2
Granulicella pectinivorans DSM 21001
Granulicella tundricola MP5ACTX9
Granulicella rosea DSM 18704
Granulicella sibirica AF10
Edaphobacter aggregans DSM 19364
Tunturibacter empetritectus M8UP20
Tunturibacter empetritectus M8UP22
Tunturibacter empetritectus M8UP23
Tunturibacter empetritectus M8UP27
Tunturibacter empetritectus M8US30
Tunturibacter gelidoferens M8UP15
Tunturibacter gelidoferens M8UP28
Tunturibacter gelidoferens M8UP30
Tunturibacter gelidoferens M8UP39
Tunturibacter lichenicola MP8S11
Tunturibacter psychrotolerans X4BP1
Tunturibacter psychrotolerans X5P2
Tunturibacter psychrotolerans X5P6
K1 Wind
K3 Wind
K6 Wind
K8 Wind
T2 Snow
T5 Snow
T6 Snow
T7 Snow

Supplementary Methods and Results

Genome analysis and description of *Tunturibacter* gen. nov. expands the diversity of *Terriglobia* in tundra soils

Adriana Messyasz, Minna K. Männistö, Lee J. Kerkhof and Max M. Häggblom

Generating Illumina short-read sequences for MP8S11, M8UP39, X5P6, and M8UP23

Sequencing was performed via 300bp paired-end Illumina MiSeq V3. Demultiplexing was done via the Illumina bcl2fastq 1.8.4 software. Adapter remnants were clipped from the reads and then reads were quality trimmed by removing reads containing more than one N, removing bases or complete reads with sequencing errors, trimming reads at 3'-end to get a minimum average Phred quality score of 10 over a window of ten bases, and removing reads with final length < 20 bases. Error correction of quality trimmed reads was conducted via Musket version 1.0.6 (k-mer size for correction: 21) (Liu *et al.*, 2013).

rRNA operon analysis

rRNA operon amplification

DNA was extracted from tundra soil isolates using the DNeasy UltraClean Microbial Kit (Qiagen) according to manufacturer's instructions. The extracted DNA from these *Acidobacteriota* isolates was used for the genome assembly (main text methods; samples M8UP23, M8UP39, and X5P6 were not included in this operon analysis). For the operon analysis bacterial ribosomal RNA (rRNA) operons were targeted via the modified 16S rRNA-27F forward primer (5' TTT CTG TTG GTG CTG ATA TTG C-[barcode overhang for PCR labeling]-AGA GTT TGA TCC TGG CTC AG 3') (Lane, 1991) and the modified 23S rRNA-2241R reverse primer (5' ACT TGC CTG TCG CTC TAT CTT C-[barcode overhang for PCR labeling]-ACC GCC CCA GTH AAA CT 3') (Hunt *et al.*, 2006; Kerkhof *et al.*, 2017). To generate ribosomal operon amplicons, these primers were added to a 25 µl PrimeStar GXL reaction with 1 µl extracted DNA, Oxford Nanopore barcodes, dNTPs, Taq polymerase, and 5X PCR buffer. Operons were then amplified with the following PCR conditions: 3 min denaturation at 94°C, 25 cycles of 10s melting at 98°C, 15s annealing at 60°C, 5 min extension at 68°C, followed by a 7min hold at 72°C. PCR product for each sample was visualized by agarose gel electrophoresis and amplicons were pooled in equimolar ratios (50 ng/sample). This pool was then cleaned with 0.5 volume of AMPure beads, 5 minute room temperature incubation, two 70% ethanol washes, and elution into 47 µl of 10mM Tris after a 5 minute room temperature incubation.

Library preparation and MinION sequencing

The operon library, consisting of operon amplicons from the isolates, was prepared for sequencing using the MinION end-repair ligation protocol LSK109 chemistry (Oxford Nanopore Technologies). Briefly, 1 µg (45 µl) of the pooled amplicons was added to 7 µl of end-repair

reaction buffer, 3 µl end-repair enzyme mix, 2.5 µl dNTPs, and brought to 60 µl with ultra-pure water. dA-tailing was done via the following conditions: 20°C for 6 minutes, 65°C for 5 minutes, cool to 4°C. dA-tailed amplicons were then bead-cleaned with 30 µl AMPure beads, followed by a 5 minute room temperature incubation, two 70% ethanol washes, and elution into 60 µl 10 mM Tris after a 5 minute room temperature incubation. Ligation was performed by transferring the bead-cleaned amplicons to a low-bind tube and then amplicons were adapter ligated by adding the following solutions sequentially: 58 µl bead-cleaned amplicon DNA, 5 µl adapter mix (AMX-F), 25 µl ligation buffer (LNB), and 12 µl blunt/TA ligation master mix. Then 2 µl of freshly prepared ATP solution (~ 4 mg/ml) was added and the mixture was incubated at room temperature for 30 minutes. A final bead-cleaned was performed by adding 40 µl of AMPure beads, 5 minute room temperature incubation, two washes with 200 µl Long Fragment Buffer (LFB), and eluted into 15 µl of elution buffer (EB) after a 5 minute room temperature incubation. 5 µl of the final bead-cleaned library was transferred to a low-bind tube and loaded onto a flongle as per the manufacturer's instructions and run with fast basecalling enabled. Once sequenced, the resulting passed reads were input into the Guppy basecaller (V 6.0.1 Oxford Nanopore Technologies). For the *Acidobacteriota* strains, a total of ~9,500 reads that passed Guppy basecalling were produced from MinION sequencing.

Operon long read consensus reconstruction

The passed reads from basecalling were then input into Geneious for quality control, demultiplexing, and long-read consensus building. Reads between 4,000-5,700bp were kept and operons from each sample were obtained by extracting the sequence in between the annotated forward and reverse MinION barcodes. All reads were inspected for size and forward orientation, reverse complementing any reads in reverse orientation. Long-read consensus construction was conducted for the 15 *Acidobacteriota* isolate samples via an iterative LastZ alignment approach (Harris, 2007). Briefly, for each *Acidobacteriota* sample, all sequences were aligned via MUSCLE (1 iteration, V 3.8.425) (Edgar, 2004) and the distance matrix was inspected to extract the 100 best aligned sequences. These sequences were divided into quarters and the last 25 were MUSCLE aligned and then inspected to extract the 10 best aligned sequences. Another MUSCLE alignment (4 iterations) of these 10 best sequences was run to create a consensus sequence. This consensus sequence was then used for a LastZ alignment (V 1.02.00) with the 10 best aligned sequences to create the first iteration of the final consensus sequence (termed "con 1A"). Con 1A was then run through a LastZ alignment with the bottom quarter of the first 100 best sequences to create the second iterative consensus sequence "Con 2A". Then each new consensus sequence iteration was LastZ aligned to each quarter of the 100 best aligned sequences, all the 100 best aligned sequences, and the first MUSCLE alignment of all sequences. This produced the final consensus with adequate coverage and length for operon annotation. The number of sequences (post Geneious demultiplexing and quality control) and final LRC length for each *Acidobacteriota* operon is recorded in Supp. Table S7. The lengths of our LRC operons spanned from ~4,200bp – 4,800bp, and the average length was ~4,767bp.

Operon annotation and phylogenetic tree analysis

We annotated the 16S rRNA, tRNA-ala, tRNA-leu, and the beginning of the 23S rRNA gene for all 15 *Acidobacteriota* isolate consensus sequences using already annotated

Acidobacteriota operons from a curated rRNA operon database (Kerkhof *et al.*, 2022). We also annotated and extracted the operons from the assemblies of the 3 isolates included in the genome analysis (M8UP23, M8UP39, and X5P6). These *Acidobacteriota* annotated operons were aligned to other known SD1 *Acidobacteriota* operons via 4 MUSCLE iterations (Edgar, 2004). The alignment was viewed and edited in Geneious to remove ambiguously aligned bases and the ITS regions between the 16S rRNA, tRNAs, and 23S rRNA genes. A phylogenetic tree of the resulting unambiguous alignment (3,905 bp) was then constructed via the maximum likelihood method (FastTree V 2.1.11 with default settings) (Price *et al.*, 2010).

56 total operons were used for the tree and the closest relative of the 15 *Acidobacteriota* operons (generated in our operon analysis) are noted in Table S6. Two of our operon isolates (M8UP14 and MP5ACTX2) were removed from the operon tree due to redundancy. In this operon tree (Supp. Fig. 1A), we see clear separation of the LRCs that group with the previously named "*Edaphobacter lichenicola*" from the other *Edaphobacter* species. We consider this a new genus of SD1 *Acidobacteriota* and name it *Tunturibacter*. Within this genus it appears that there are at least 4 species, each with several strains as seen in Fig. S1B. It also appears that *Granulicella mallensis, G. paludicola,* and *G. cerasi* that group with *Bryocella elongata* are clustering separately from the other *Granulicella* species and may represent a separate genus as well (Fig. S1A). This tree had similar topology to a 16S rRNA tree (Fig. S2A) constructed with the same method (unambiguous MUSCLE alignment of the 16S rRNA region – 1,419bp - and FastTree construction) using 62 *Acidobacteriota* species/strains (not including redundant M8UP14 and MP5ACTX2). The 16S rRNA gene sub-tree also separates the 4 new species within the proposed *Tunturibacter* genus (Fig. S2B).

Bacterial single copy genes used via GToTree

The 74 bacterial single copy genes used for phylogenetic analysis via GToTree are available for download at: https://zenodo.org/record/7860735/files/Bacteria.hmm?download=1

The pfam names of these SCGs are:
5-FTHF_cyc-lig, Adenylsucc_synt, ADK, AICARFT_IMPCHas, ATP-synt, ATP-synt_A, Chorismate_synt, EF_TS, eIF-1a, Exonuc_VII_L, Exonuc_VII_S, GrpE, Ham1p_like, IPPT, OSCP, Peptidase_A8, Pept_tRNA_hydro, PGK, PseudoU_synth_1, RBFA, RecO_C, Ribonuclease_P, Ribosomal_L1, Ribosomal_L13, Ribosomal_L14, Ribosomal_L16, Ribosomal_L17, Ribosomal_L18p, Ribosomal_L19, Ribosomal_L20, Ribosomal_L21p, Ribosomal_L22, Ribosomal_L23, Ribosomal_L24, Ribosomal_L27, Ribosomal_L27A, Ribosomal_L28, Ribosomal_L29, Ribosomal_L3, Ribosomal_L32p, Ribosomal_L34, Ribosomal_L35p, Ribosomal_L4, Ribosomal_L6, Ribosomal_L9_C, Ribosomal_S10, Ribosomal_S11, Ribosomal_S13, Ribosomal_S15, Ribosomal_S16, Ribosomal_S17, Ribosomal_S19, Ribosomal_S2, Ribosomal_S20p, Ribosomal_S6, Ribosomal_S7, Ribosomal_S8, Ribosomal_S9, Ribosom_S12_S23, RNA_pol_L, RNA_pol_Rpb6, RRF, RsfS, RuvX, SecE, SecG, SecY, SmpB, tRNA-synt_1d, tRNA_m1G_MT, TsaE, UPF0054, YajC, and YidD

References

Edgar, R.C. (2004) MUSCLE: a multiple sequence alignment method with reduced time and space complexity. *BMC Bioinformatics* **5**: 113.

Harris, R.S. (2007) Improved pairwise alignment of genomic DNA. PhD thesis.

Hunt, D.E., Klepac-Ceraj, V., Acinas, S.G., Gautier, C., Bertilsson, S., and Polz, M.F. (2006) Evaluation of 23S rRNA PCR Primers for Use in Phylogenetic Studies of Bacterial Diversity. *Applied and Environmental Microbiology* **72**: 2221–2225.

Kerkhof, L.J., Dillon, K.P., Häggblom, M.M., and McGuinness, L.R. (2017) Profiling bacterial communities by MinION sequencing of ribosomal operons. *Microbiome* **5**: 116.

Kerkhof, L.J., Roth, P.A., Deshpande, S.V., Bernhards, R.C., Liem, A.T., Hill, J.M., et al. (2022) A ribosomal operon database and MegaBLAST settings for strain-level resolution of microbiomes. *FEMS Microbes* **3**: xtac002.

Lane, D.J. (1991) 16S/23S rRNA sequencing. In *16S/23S rRNA sequencing*. Chichester, England: John Wiley & Sons Ltd., pp. 115–175.

Liu, Y., Schröder, J., and Schmidt, B. (2013) Musket: a multistage k-mer spectrum-based error corrector for Illumina sequence data. *Bioinformatics* **29**: 308–315.

Price, M.N., Dehal, P.S., and Arkin, A.P. (2010) FastTree 2 – Approximately Maximum-Likelihood Trees for Large Alignments. *PLOS ONE* **5**: e9490.

Supplementary Tables and Figures

Genome analysis and description of *Tunturibacter* gen. nov. expands the diversity of *Terriglobia* in tundra soils

Adriana Messyasz, Minna K. Männistö, Lee J. Kerkhof and Max M. Häggblom

Supplementary Table S1. Genome assemblies.

Supplementary Table S2. Plasmid database highest identity hit for second longest contig in genome assemblies.

Supplementary Table S3. Accession numbers for NCBI genomes.

Supplementary Table S4. Phenotypic data for *Tunturibacter* strains.

Supplementary Table S5. Enriched genes from the enriched functional pathways within the *Tunturibacter* species.

Supplementary Table S6. NCBI Accession numbers for *Tunturibacter* gen. nov. 16S rRNA genes and genomes.

Supplementary Table S7. Operon long read consensus (LRC) data.

Supplementary Figure S1A. rRNA operon phylogeny (accession numbers for genomes taken from NCBI are in Supp. Table S2).

Supplementary Figure S1B. rRNA operon phylogeny of novel *Tunturibacter* genus (accession numbers for genomes taken from NCBI are in Supp. Table S2).

Supplementary Figure S2A. 16S rRNA gene phylogeny (accession numbers for genomes taken from NCBI are in Supp. Table S2).

Supplementary Figure S2B. 16S rRNA gene phylogeny of novel *Tunturibacter* species (accession numbers for genomes taken from NCBI are in Supp. Table S2).

Supplementary Figure S3. Orthogroup phylogeny (accession numbers for genomes taken from NCBI are in Supp. Table S2).

Supplementary Figure S4. Mauve genome comparison.

Supplementary Figure S5. Distribution of major CAZy family genes (% of total predicted genes).

Supplementary Figure S6. Colony morphology and photomicrographs of *Tunturibacter* strains.

Supplementary Table S1. Genome assemblies.

Strain	Total MinION reads	Total basecalled reads	Trycycler output total bp	Trycyler contigs	Trycycler completeness	Trycycler contamination	Polypolish output total bp	Polypolish contigs	Polished completeness	Polished contamination	Illumina reads (R1)	Illumina reads source	GTDB relative, closest ANI, AA % in MSA
M8UP30	99,451	57,516	5,287,291	2	90.52	0.86	5,289,310	2	100.00	0.86	10,793,290	JGI: Edaphobacter lichenicola M8UP30 (Project ID: 1254311)	GCF_013410115.1 Edaphobacter lichenicola, 100, 93.33
MP5ACTX2	160,979	55,460	5,590,690	6	95.52	0.86	NA	NA	NA	NA	NA	NA	GCF_013410065.1 Granulicella B arctica, 79.66, 86.96
M8UP20	63,710	41,308	4,908,185	2	89.31	0.00	NA	NA	NA	NA	NA	NA	GCF_014201315.1 Edaphobacter lichenicola, 99.89, 76.45
M8UP27	118,141	33,801	4,896,458	2	89.66	0.86	4,897,989	2	100.00	0.05	5,117,144	JGI: Edaphobacter lichenicola M8UP27 (Project ID: 1254301)	GCF_014201315.1 Edaphobacter lichenicola, 100, 93.33
M8UP28	123,689	71,052	6,830,749	2	91.42	0.86	NA	NA	NA	NA	NA	NA	GCF_013410115.1 Edaphobacter lichenicola, 89.77, 80.9
X4BP1	71,590	50,435	6,127,097	1	91.21	0.86	6,129,460	1	100.00	0.86	7,169,664	JGI: Edaphobacter lichenicola X4BP1 (Project ID: 1254307)	GCF_014201335.1 Edaphobacter lichenicola, 90.93, 91.74
X5P3	222,828	63,146	6,506,373	1	93.07	2.63	6,509,459	1	100.00	2.63	5,630,000	JGI: Granulicella mallensis X5P3 (Project ID: 1254317)	GCF_014203225.1 Granulicella mallensis A, 100, 94.12
X4EP2	733,456	71,8215	4,305,473	1	96.58	1.71	4,305,847	1	100.00	1.71	6,319,706	JGI: Granulicella arctica X4EP2 (Project ID: 1254323)	GCF_013410065.1 Granulicella B arctica, 100, 93.91
MP8S11	122,775	86,931	6,273,739	2	88.84	1.90	6,275,948	2	100.00	1.72	536,285	Previous assembly	GCF_014201335.1 Edaphobacter lichenicola, na, 92.97
M8UP22	53,858	38,398	5,088,737	2	93.17	0.43	5,091,646	2	99.78	0.00	6,776,254	JGI: Edaphobacter lichenicola M8UP22 (Project ID: 1254299)	GCF_013410875.1 Edphobacter lichenicola, 100, 94.06
M8UP39	22,410	15,636	5,579,037	2	94.83	0.86	5,581,845	2	100.00	0.86	901,687	Previous SPAdes assembly	GCF_013410115.1 Edaphobacter lichenicola, 98.07, 93.31
X5P6	43,422	24,621	5,633,542	2	91.16	0.86	5,636,298	2	100.00	0.86	896,994	Previous SPAdes assembly	GCF_014201335.1 Edaphobacter lichenicola, 90.3, 92.5
M8UP23	61,597	39,643	5,027,926	3	94.49	0.00	5,030,191	3	99.78	0.00	815,655	Previous SPAdes assembly	GCF_013410875.1 Edaphobacter lichenicola, 98.51, 94.08

Supplementary Table S2. Plasmid database highest identity hit for second longest contig in genome assemblies.

	Plasmid Database Hit Result			
Genome	**% Identity**	**P-value**	**Plasmid Taxonomy**	**Plasmid length (bp)**
M8UP23	75.83	2.93e-15	Granulicella tundricola MP5ACTX9 plasmid pACIX903	188,167
M8UP22	74.38	5.66e-12	Paracoccus aminovorans isolate JCM7685 plasmid III	4,158
M8UP27	74.38	7.09e-11	Granulicella tundricola MP5ACTX9 plasmid pACIX903	188,167
M8UP20	75.83	1.01e-15	Granulicella tundricola MP5ACTX9 plasmid pACIX903	188,167
M8UP39	74.38	4.26e-10	Granulicella tundricola MP5ACTX9 plasmid pACIX903	188,167
M8UP30	74.38	5.11e-10	Granulicella tundricola MP5ACTX9 plasmid pACIX903	188,167
M8UP28	74.38	1.33e-9	Granulicella tundricola MP5ACTX9 plasmid pACIX903	188,167
X5P6	71.97	3.81e-06	Sphingobium xenophagum QYY plasmid pSx-Qyy	5,683
MP8S11	74.38	1.32e-8	Granulicella tundricola MP5ACTX9 plasmid pACIX904	115,493
MP5ACTX2	82.36	4.31e-94	Granulicella tundricola MP5ACTX9 plasmid pACIX905	115,221

Supplementary Table S3. Accession numbers for NCBI genomes.

Acidobacteriota	Genome accession num.	16S accession num.
Acidicapsa acidiphila MCF10	n/a	NR_148579.1
Acidicapsa acidisoli SK11	GCF_025685625.1	NR_148580.1
Acidicapsa borealis KA1	n/a	NR_117182.1
Acidicapsa dinghuensis 4GSKX	GCF_025685685.1	NR_179686.1
Acidicapsa ferrireducens MCF9	n/a	NR_149202.1
Acidicapsa ligni WH120	GCF_025685655.1	NR_116444.1
Acidipila rosea DSM 103428	GCF_004339725.1	n/a
Acidisarcina polymorpha SBC82	GCF_003330725.1	NR_180095.1
Acidobacteriaceae bacterium KBS 83	GCF_000381585.1	n/a
Acidobacteriaceae bacterium KBS 89	GCF_000381605.1	n/a
Acidobacterium capsulatum ATCC 51196	GCF_000022565.1	NR_074106.1
Alloacidobacterium dinghuense 4Y35	GCF_014274465.1	NR_181376.1
Bryocella elongata DSM 22489	GCF_900108185.1	n/a
Chloracidobacterium thermophilum B	GCF_018304665.1	NR_074296.1
Edaphobacter acidisoli CGMCC	GCF_014642855.1	n/a
Edaphobacter aggregans DSM 19364	GCF_000745965.1	n/a
Edaphobacter bradus 4MSH08	GCF_025685645.1	NR_179685.1
Edaphobacter dinghuensis DHF9	GCF_025685705.1	NR_147748.1
Edaphobacter flagellatus HZ411	GCF_025264665.1	NR_179102.1
Edaphobacter modestus DSM 18101	GCF_004217555.1	n/a
Granulicella acidiphila MCF40	n/a	NR_148567.1
Granulicella aggregans M8UP14	GCF_014203275.1	n/a
Granulicella arctica DSM 23128	GCF_025685605.1	n/a
Granulicella cerasi Sakura1	GCF_025685575.1	NR_134047.1
Granulicella mallensis MP5ACTX8	GCF_000178955.2	n/a
Granulicella paludicola OB1010	GCF_025685545.1	NR_115072.1
Granulicella pectinivorans DSM 21001	GCF_900114625.1	n/a
Granulicella rosea DSM 18704	GCF_900188085.1	n/a
Granulicella sapmiensis S6CTX5A	n/a	NR_118023.1
Granulicella sibirica AF10	GCF_004115155.1	NR_180238.1
Granulicella tundricola MP5ACTX9	GCF_000178975.2	NR_118021.1
Koribacter versatilis Ellin 345	GCF_000014005.1	n/a
Occallatibacter riparius DSM 25168	GCF_025264625.1	n/a
Occallatibacter savannae AB23	GCF_003131205.1	n/a
Paracidobacterium acidisoli 4G-K13	GCF_003428625.2	NR_179684.1
Pseudacidobacterium ailaaui PMMR2	GCF_000688455.1	NR_153719.1
Silvibacterium bohemicum DSM 103733	GCF_014201455.1	n/a
Silvibacterium dinghuense DHOF10	GCF_004123295.1	NR_147722.1
Telmatobacter bradus TPB6017	n/a	NR_115074.1
Terracidiphilus gabretensis S55	GCF_001449115.1	NR_146368.1
Terriglobus albidus ORNL	GCF_008000815.1	n/a
Terriglobus aquaticus 03SUJ4	GCF_025685415.1	NR_135733.1
Terriglobus roseus DSM 18391	GCF_000265425.1	n/a
Terriglobus saanensis SP1PR4	GCF_000179915.2	NR_117834.1
Terriglobus tenax DRP 35	GCF_025685395.1	NR_133877.1
Tunturibacter empetritectus M8US30	GCF_014201375.1	n/a
Tunturibacter gelidoferens M8UP15	GCF_014201365.1	n/a
Tunturibacter lichenicola DSM 104462	GCF_025264645.1	n/a
Tunutribacter psychrotolerans X5P2	GCF_014201335.1	n/a

Supplementary Table S4. Phenotypic data for *Tunturibacter* strains.

Phentopyic Data	M8UP23	M8UP39	X5P6	T. lichenicola (Dedysh et al., 2018)
Hydrolysis of polysaccharides				
CMC	-	w	w	
Xylan	+	+	-	+
Pectin	+	+	+	-
Lichenin	-	+	+	+
Starch	-	w	+	-
Xanthan	+	-	+	
Gum arabic	+	w	+	
API ZYM tests				
Alkaline phosphatase	+	+	+	+
Esterase (C4)	+	+	-	+
Esterase (C8)	-	+	+	+
Lipase (C14)	-	-	-	-
Leucine arylamidase	+	+	+	+
Valine arylamidase	+	+	+	+
Cystine arylamidase	+	+	+	+
Trypsin	-	-	+	-
a-chymotrypsin	-	-	+	+
Acid phosphatase	+	+	+	+
Naphtol-AS-BI-phophohydrolase	+	+	+	+
α-galactosidase	+	+	+	+
β-galactosidase	+	+	+	+
β-glucuronidase	+	+	+	+
α-glucosidase	+	+	+	+
β-glucosidase	+	+	+	+
N-acetyl-b-glucosaminidase	+	+	+	+
α-mannosidase	-	-	-	-
α-fucosidase	+	-	-	-
Quinones				
	MK-8	MK-8	MK-8	MK-8
Major cellular fatty acids				
	i-15:0, i-13:0, 16:1$_{\omega}$7c, 16:0	i-15:0, i-13:0, 16:1$_{\omega}$7c, 16:0	i-15:0, i-13:0, 16:1$_{\omega}$7c, 16:0	

+: positive reaction, - : negative reaction, w : weak positive reaction

Supplementary Table S5. Enriched genes from the enriched functional pathways within the *Tunturibacter* species.

KEGG Module	Accession	Genes
Aromatic amino acid metabolism: Tryptophan metabolism	M00038; M00912	Selenocysteine lyase/Cysteine desulfurase (CsdA); Tryptophan 2,3-dioxygenase (vermilion) (TDO2); Kynurenine formamidase
Amino acid metabolism: Betaine biosynthesis	M00555; M00032; M00135	Acyl-CoA reductase or other NAD-dependent aldehyde dehydrogenase (AdhE)
COG20 Pathway	**Accession**	**Genes**
Menaquinone biosynthesis	COG0318	O-succinylbenzoic acid-CoA ligase MenE or related acyl-CoA synthetase (AMP-forming) (MenE/FadK)
Lysine biosynthesis	COG3320	Thioester reductase domain of alpha aminoadipate reductase Lys2 and NRPSs (Lys2b)
Cobalamin/B12 biosynthesis	COG1010; COG2243	Precorrin-3B methylase; Precorrin-2 methylase
Pyrimidine salvage	COG0402	Cytosine/adenosine deaminase or related metal-dependent hydrolase
Biotin biosynthesis	COG2226	Ubiquinone/menaquinone biosynthesis C-methylase UbiE/MenG
Molybdopterin biosynthesis	COG0314; COG1977	Molybdopterin synthase catalytic subunit MoaE; Molybdopterin synthase sulfur carrier subunit MoaD

Supplementary Table S6. NCBI Accession numbers for *Tunturibacter* gen. nov. 16S rRNA genes and genomes

Tunturibacter species	16S rRNA gene accession	Genome accession	Genome Localid
Tunturibacter lichenicola MP8S11	OR449317	CP132944-CP132945	SAMN36939420
Tunturibacter empetritectus M8UP23	OR449309	CP132932-CP132934	SAMN36939426
Tunturibacter empetritectus M8UP20	OR449312	CP132926-CP132927	SAMN36939429
Tunturibacter empetritectus M8UP22	OR449313	CP132930-CP132931	SAMN36939427
Tunturibacter empetritectus M8UP27	OR449314	CP132928-CP132929	SAMN36939428
Tunturibacter gelidoferens M8UP39	OR449311	CP132937-CP132938	SAMN36939424
Tunturibacter gelidoferens M8UP28	OR449315	CP132939-CP132940	SAMN36939423
Tunturibacter gelidoferens M8UP30	OR449316	CP132935-CP132936	SAMN36939425
Tunturibacter psychrotolerans X5P6	OR449310	CP132942-CP132943	SAMN36939421
Tunturibacter psychrotolerans X4BP1	OR449318	CP132941	SAMN36939422

Supplementary Table S7. Operon long read consensus (LRC) data.

Strain	Geneious filtered reads	LRC length (bp)	Closest relative
M8UP22	629	4799	Edaphobacter lichenicola DSM 104462 (GCF_025264645.1)
M8UP27	802	4825	Edaphobacter lichenicola DSM 104462 (GCF_025264645.1)
M8UP20	773	4828	Edaphobacter lichenicola DSM 104462 (GCF_025264645.1)
M8US30	635	4824	Edaphobacter lichenicola DSM 104462 (GCF_025264645.1)
MP8S11	643	4801	Edaphobacter lichenicola DSM 104462 (GCF_025264645.1)
X4BP1	795	4825	Edaphobacter lichenicola DSM 104462 (GCF_025264645.1)
M8UP28	521	4795	Edaphobacter lichenicola DSM 104462 (GCF_025264645.1)
M8UP30	336	4829	Edaphobacter lichenicola DSM 104462 (GCF_025264645.1)
X5P2	1,005	4808	Edaphobacter lichenicola DSM 104462 (GCF_025264645.1)
M8UP15	503	4810	Edaphobacter lichenicola DSM 104462 (GCF_025264645.1)
X5P3	786	4800	Granulicella mallensis MP5ACTX8 (GCF_000178955.2)
M8UP14	739	4812	Granulicella aggregans M8UP14 (GCF_014203275.1)
MP5ACTX2	274	4187	Granulicella arctica DSM 23128 (GCF_025685605.1)
M8US31	435	4808	Granulicella arctica DSM 23128 (GCF_025685605.1)
X4EP2	713	4751	Granulicella arctica DSM 23128 (GCF_025685605.1)

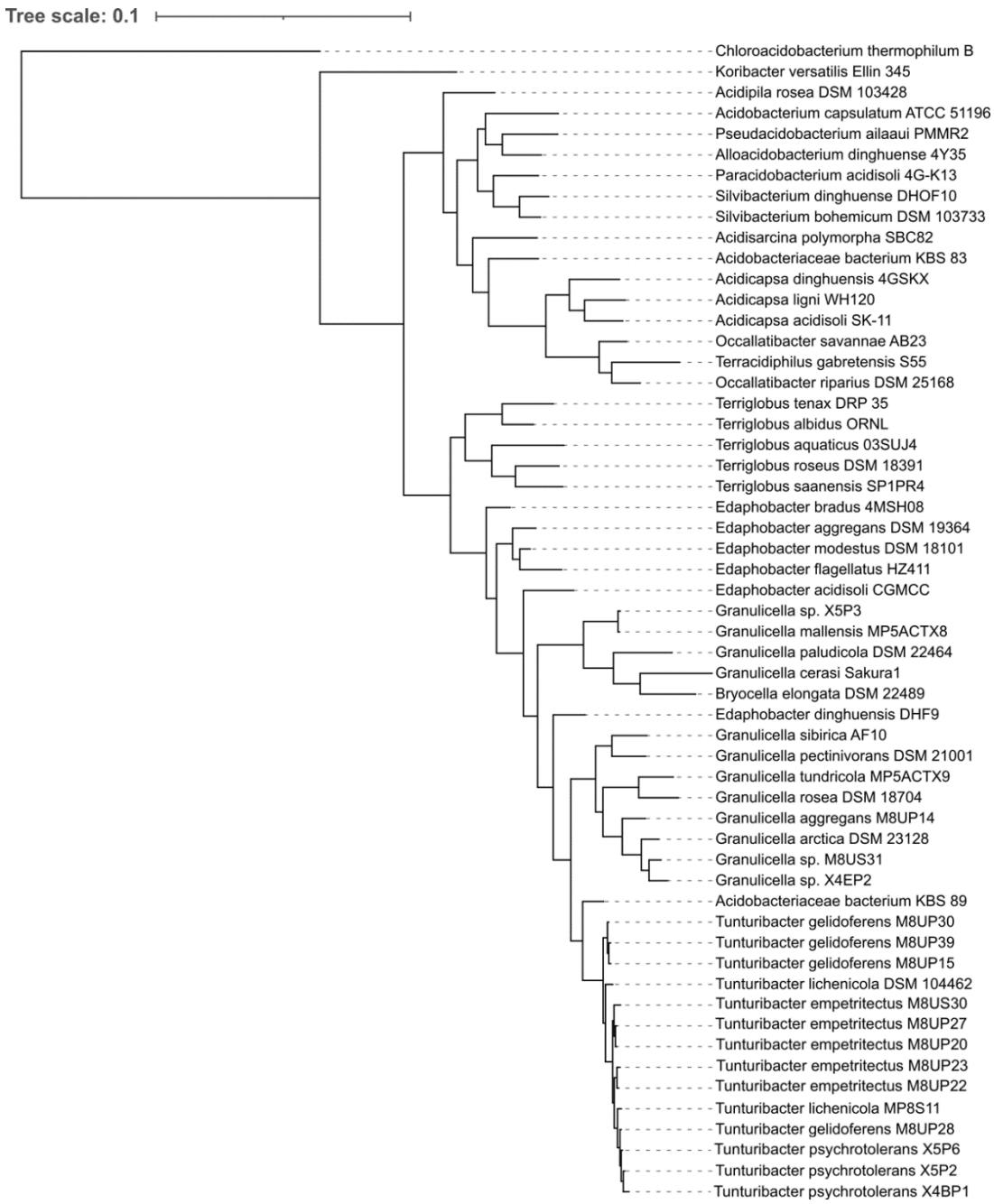

Supplementary Figure S1A. rRNA operon phylogeny (accession numbers for genomes taken from NCBI are in Supp. Table S2).

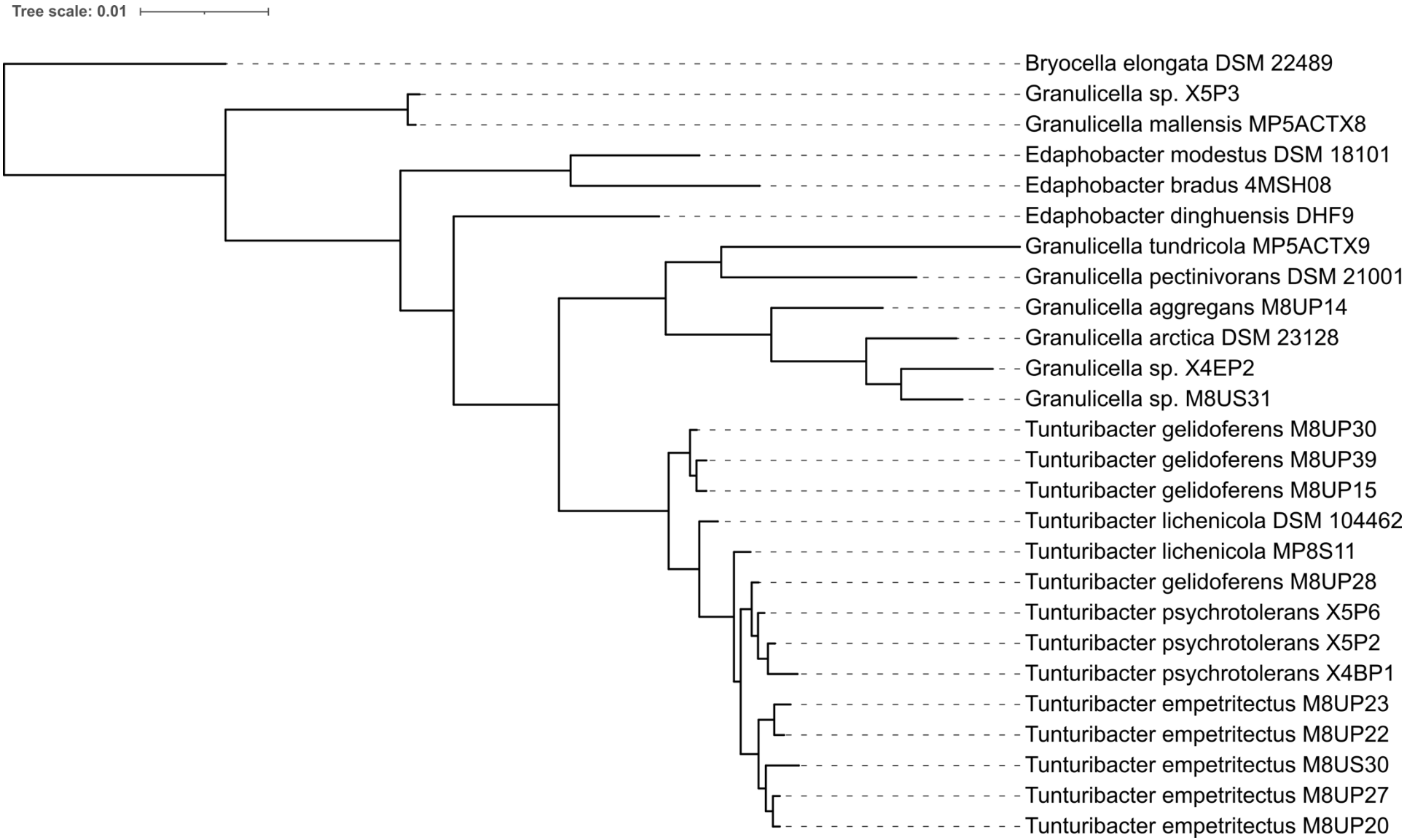

Supplementary Figure S1B. rRNA operon phylogeny of novel *Tunturibacter* genus (accession numbers for genomes taken from NCBI are in Supp. Table S2).

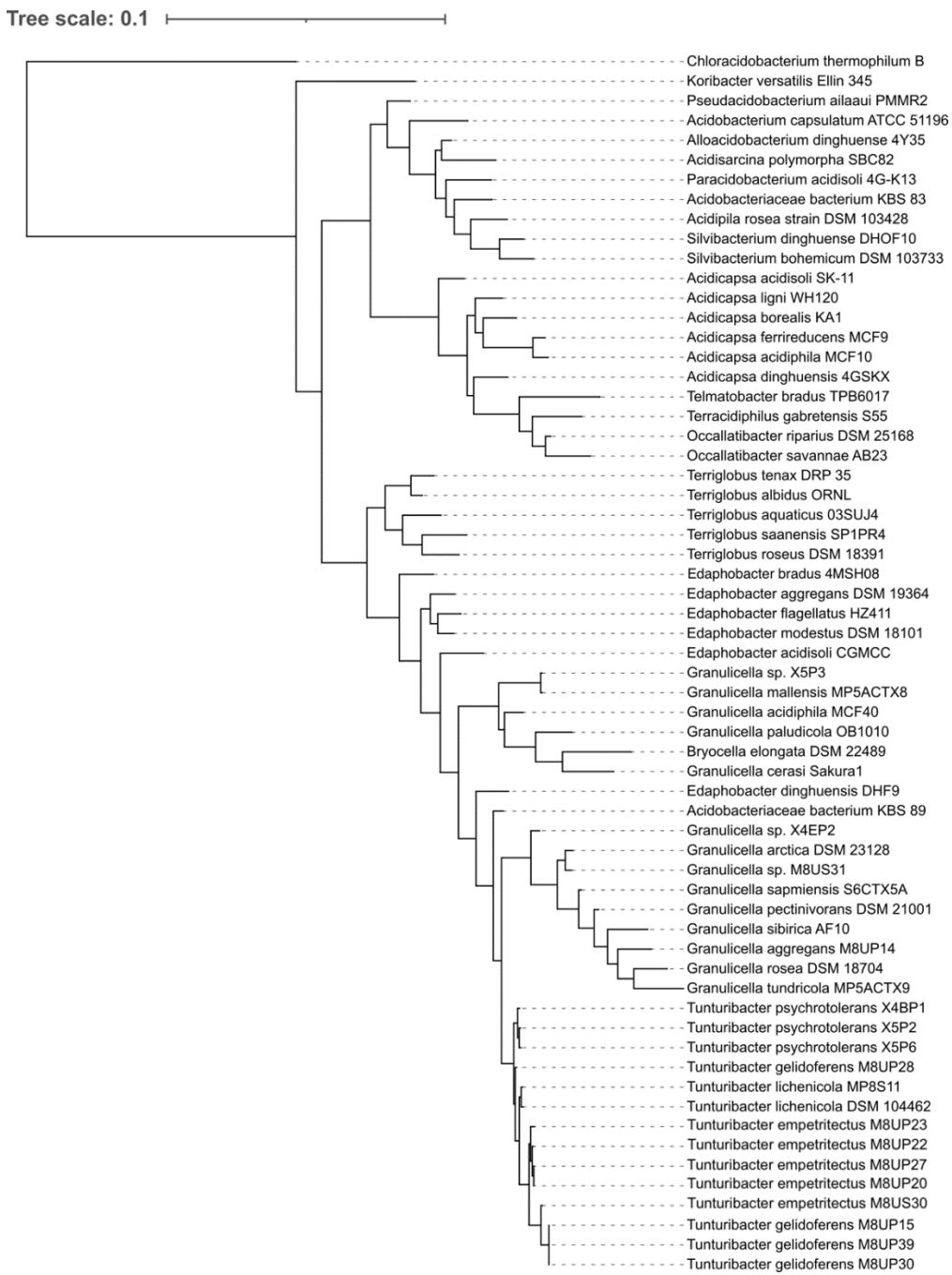

Supplementary Figure S2A. 16S rRNA gene phylogeny (accession numbers for genomes taken from NCBI are in Supp. Table S2).

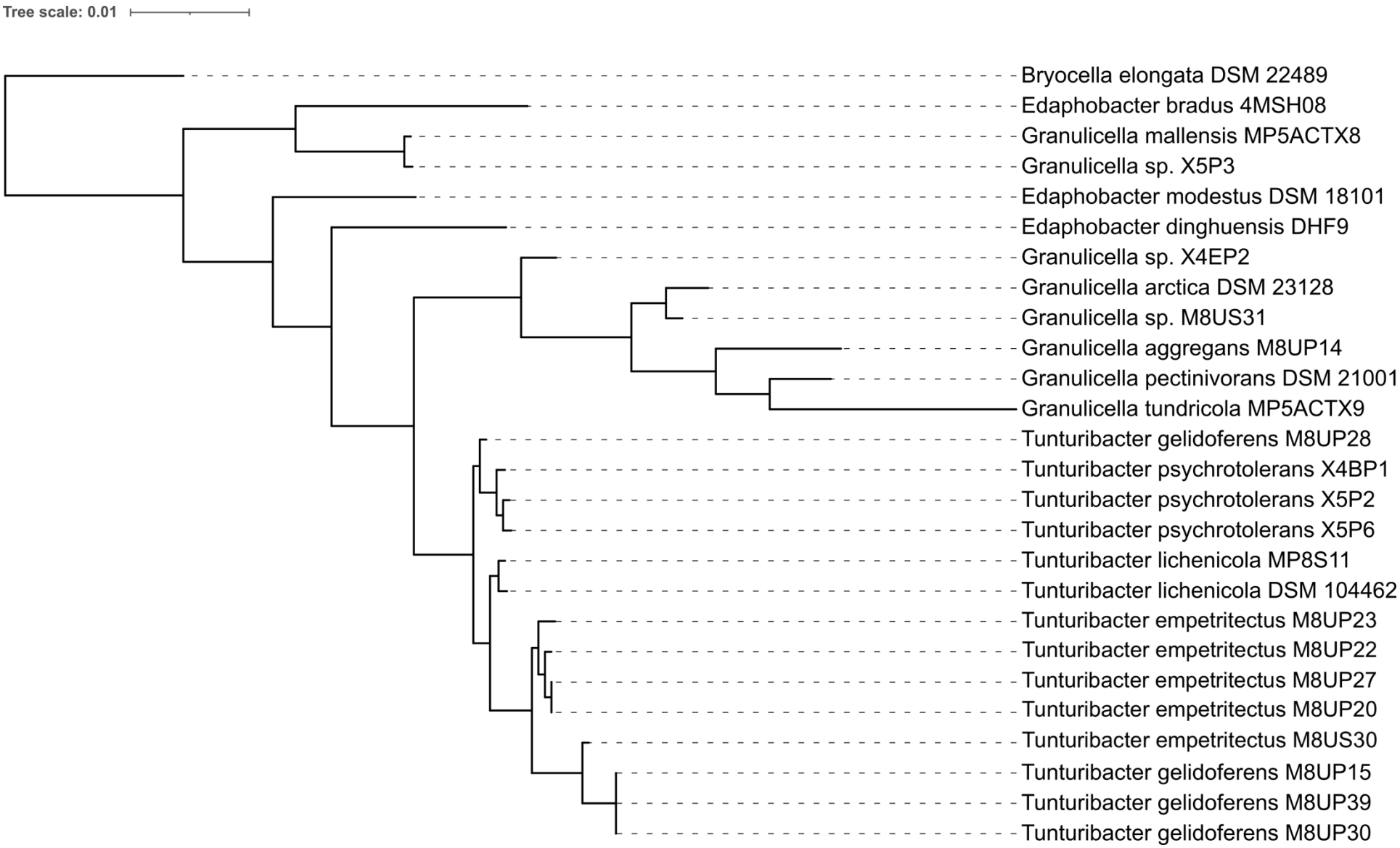

Supplementary Figure S2B. 16S rRNA gene phylogeny of novel *Tunturibacter* species (accession numbers for genomes taken from NCBI are in Supp. Table S2).

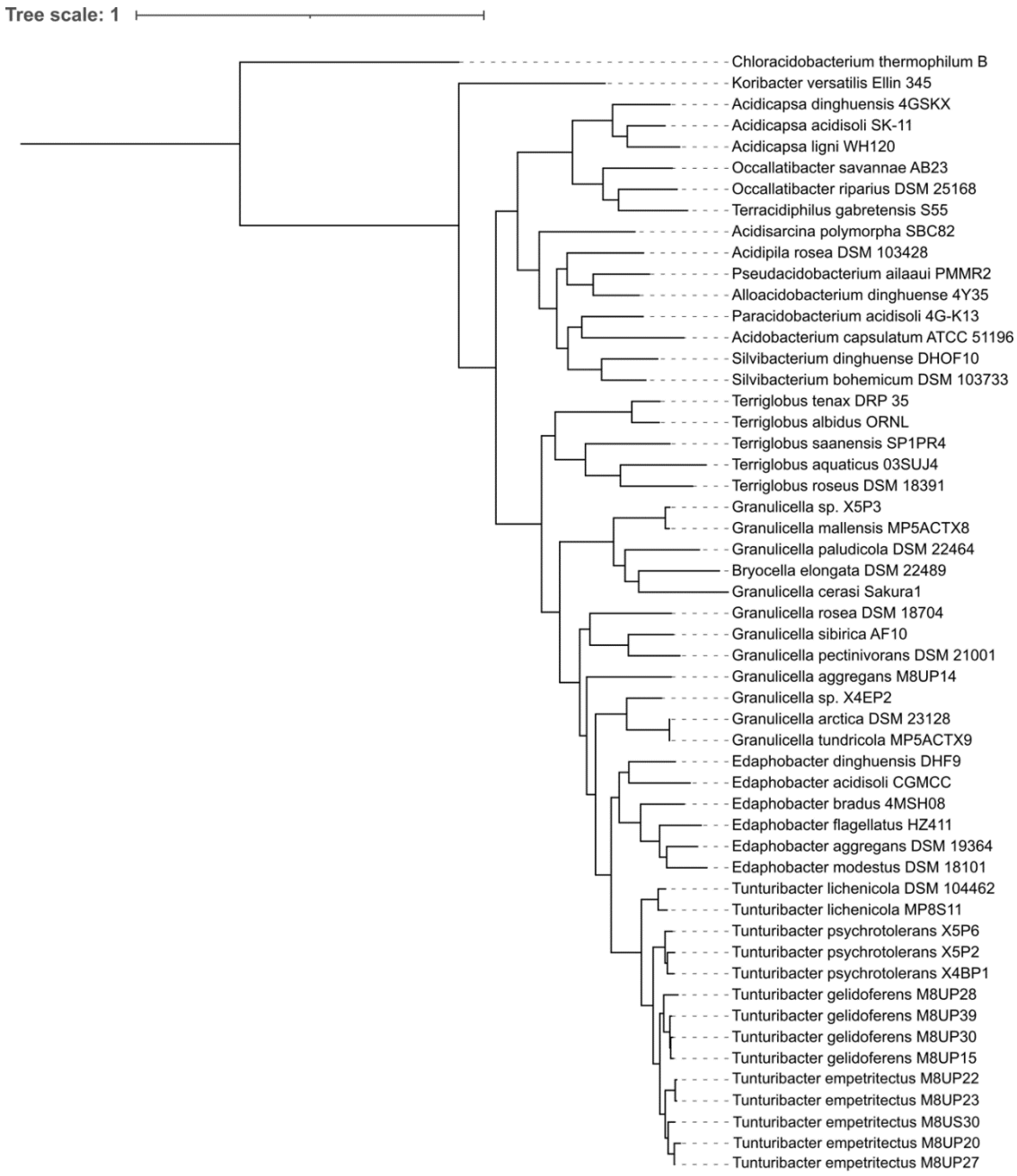

Supplementary Figure S3. Orthogroup phylogeny (accession numbers for genomes taken from NCBI are in Supp. Table S2).

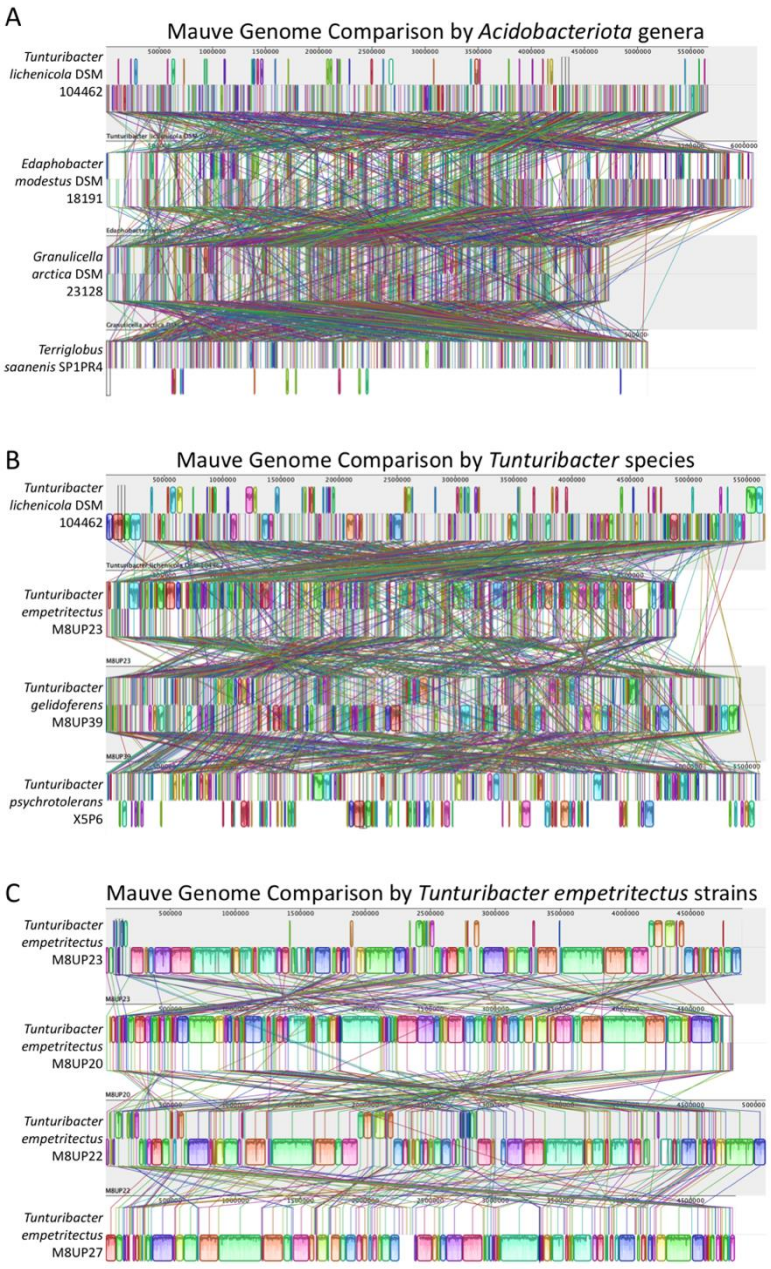

Supplementary Figure S4. Mauve genome comparison.

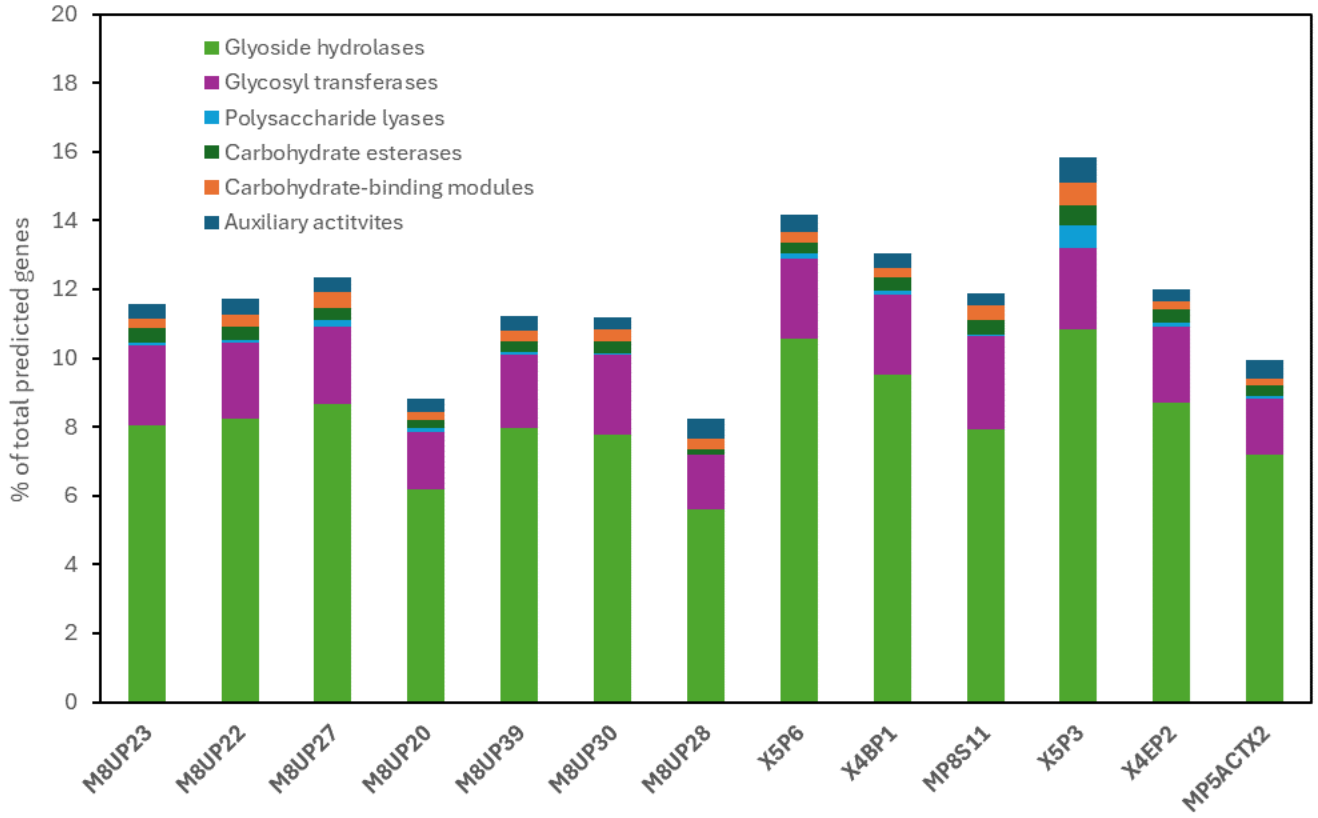

Supplementary Figure S5. Distribution of major CAZy family genes (% of total predicted genes): glycoside hydrolases, glycosyl transferases, polysaccharide lyases, carbohydrate esterases, and noncatalytic carbohydrate-binding modules in the genomes of tundra *Acidobacteriota* strains.

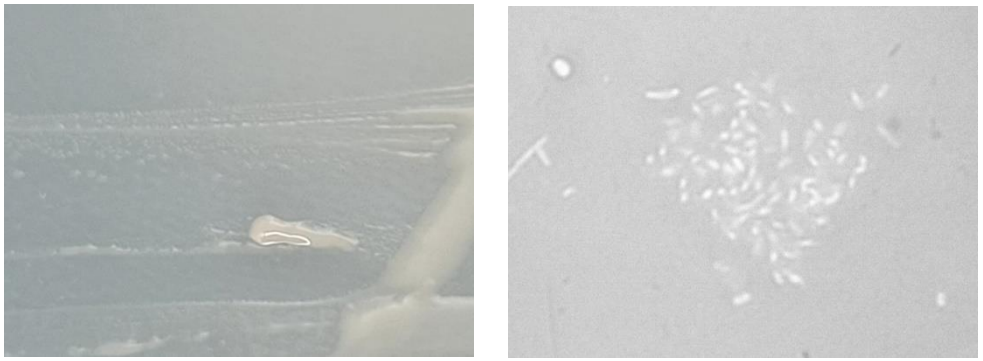

Tunturibacter empetritectus M8UP23^{T}

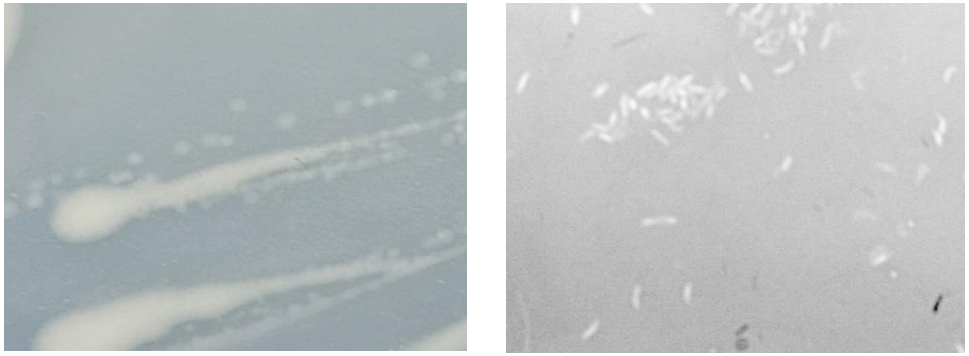

Tunturibacter gelidoferens M8UP39^{T}

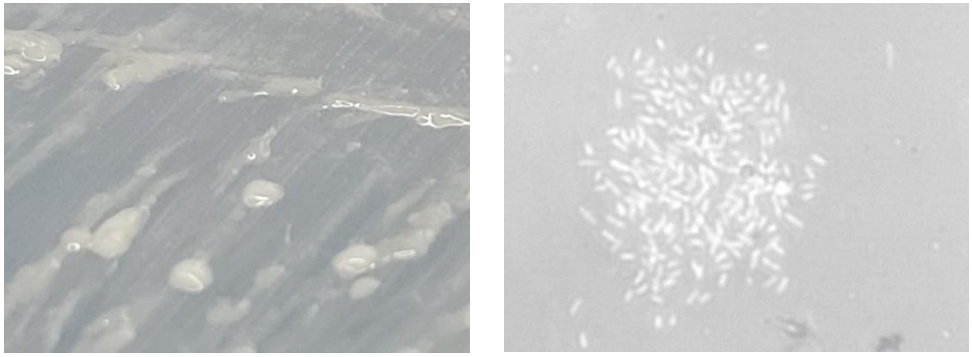

Tunturibacter psychrotolerans X5P6^{T}

Supplementary Figure S6. Colony morphology (left) and photomicrographs (right) of *Tunturibacter* strains.

Cultures were grown for ~1 week on GY medium containing glucose (1 g l^{-1}) and yeast extract (0.5 gl-1) in VL55. Negative staining by eosin-nigrosin and viewed at 1000X magnification.